TECHNISCHE UNIVERSITÄT WIEN
Vienna University of Technology

MASTERARBEIT

Monitoring and simulation of the thermal impact of sun-shading systems

ausgeführt zum Zwecke der Erlangung des akademischen Grades
eines Diplom-Ingenieurs

unter der Leitung von
Univ.-Prof. Dipl.-Ing. Dr.techn. Ardeshir Mahdavi
E 259-3 Abteilung für Bauphysik und Bauökologie
Institut für Architekturwisenschaften

eingereicht an der
Technischen Universität Wien
Fakultät für Architektur und Raumplanung

von

Aurelien Bres
Matrikelnr. 1127866

Wien, im November 2013

Kurzfassung

Die folgende Diplomarbeit befasst sich mit der Bewertung der thermischen Wirkungen von Sonnenschutzsystemen. Abschattungseinrichtungen können sommerliche Überwärmung in Gebäuden abmildern und/oder die Kühllasten verringern. Dynamische Gebäudesimulation und Monitoring ergänzen sich gegenseitig bei der Ermittlung dieser Wirkungen. Hier werden diese Methoden auf einen Büroraum mit zwei Südfenstern angewendet. Das Monitoring ermöglicht die Kalibrierung der Gebäudesimulation. Dabei wird zwischen gemessenen und simulierten Stundenwerten der Innentemperatur eine bessere Übereinstimmung erzielt. Wiederum begründet die Simulation die Wahl von zwei Sonnenschutzsystemen, Außen- und Innenjalousien, deren Auswirkungen auf das Raumklima nacheinander überwacht werden. Schließlich wird die Simulation der Sonnenschutzwirkung auch kalibriert. Dadurch werden die Simulationsergebnisse grundsätzlich bestätigt. Es wird insbesondere gezeigt, dass Außenjalousien einen wirkungsvolleren Schutz gegen sommerliche Überwärmung bieten.

Summary

This Master's Thesis deals with the evaluation of the thermal effects of sun-shading systems. Shading devices can contribute to the attenuation of sommerly overheating and/or to the reduction of space cooling loads. With the example of an office room with two south facing windows, it is attempted to show that dynamic building simulation and monitoring are two complementary means of quantifying these effects. Simulation is calibrated with the help of the values obtained by monitoring in the office room and two adjacent spaces. This results in a better match between the hourly values of measured and simulated temperatures. The simulation of different shading systems motivates the choice of two of them, consisting in external and internal Venetian blinds. These are then successively applied to the room windows, and their effects are monitored and compared to the simulation. Measured data allows the simulation results to be confirmed and made more accurate. In particular, the better performance of external blinds with regard to the protection against overheating is confirmed.

Acknowledgments

First of all, I would like to express my gratitude to my supervisor, Professor Dr. Ardeshir Mahdavi, as well as to Dr.techn. Matthias Schuss, Farhang Tahmasebi and the whole team of the Department of Building Physics and Human Ecology.

I heartily thank my family and my flatmates, especially Eleonora.

Contents

Chapter 1

Introduction

1.1 Motivation

In a global context of increasingly important challenges linked to energy consumption, the building sector plays a significant role. In the European Union, in 2004, buildings accounted for 37% of final energy consumption (Perez-Lombard et al. 2008), of which more than half for space conditioning. This energy consumption also has a considerable impact on climate change (Levermore, 2008).

While energy efficiency policies and thermal insulation result in lower heating energy demand, the amount of energy required for space cooling seems to be on the rise. For similar reasons, summer overheating in buildings is also a growing issue.

The use of shading is a key element in coping with these issues, solar radiation being a paramount factor in overheating during warm periods. An appropriate shading system should be adapted to the orientation and different conditions of the shaded building part. It also requires taking into account dynamic phenomena, with important variations during a single day. Thus, detailed dynamic simulation seems to be necessary for the evaluation of the effects of shading systems on the thermal behaviour of buildings. Concurrently, monitoring can help justify and tune dynamic simulation. Thus, this work aims at investigating the potential of both monitoring and dynamic building simulation in the evaluation of sun shading systems.

1.2 Objective

This Master's thesis focuses on the evaluation of the effects of dynamic shading devices on the thermal behaviour of buildings, using both dynamic building simulation and building monitoring. Monitoring of a room at the Technical University of Vienna allows us to get real-life data about the effects of internal and external blinds on the interior climate, and to calibrate a dynamic simulation. The simulation in turn should give an understanding of the physical phenomena, and make extrapolation possible. Calculations of annual heating and cooling energy demands, overheating and maximal cooling load can be compared for different shading systems. The objective of this work is to evaluate the thermal effects of two louvered shading devices, as well as to determine how far the combination of monitoring and calibrated dynamic simulation makes this possible.

1.3 Thesis Structure

This master's thesis is structured in six sections. After the introduction, the second section gives background information about shading systems and their physical principles, dynamic building simulation and building monitoring. The third section speficies the methodology, which is based on the association of simulation and monitoring of a room. The simulation and calibration methodology is adapted to the specific dynamic simulation tool, EDSL Tas. The results from these complementary approaches are then discussed in section 4.

Chapter 2

Background

2.1 Shading systems

In the following, background information is given on energy transfers in glazed areas, on shading devices, and how they influence these energy transfers.

2.1.1 Energy transfer in glazed areas

Thermal conduction is usually the dominant form of heat transport in opaque constructions. Thus, the thermal transmittance, or U-value, gives the most important information about heat transport through a non-glazed building part. In its calculation, convection is only taken into account as boundary condition, or represented by a heat transfer coefficient.

On the other hand, glazed areas are subject to several interacting types of energy transfer. In particular, they represent the main access for solar radiation in buildings. Solar radiation and heat transfers without solar radiation are often treated separately, as in the next two paragraphs.

Solar radiation

Solar radiation is the electromagnetic radiation given off by the Sun. It is composed of different frequency ranges, each of which is differently filtered through the atmosphere before reaching a surface. Visible light is the portion of this electromagnetic radiation with a wagelength between 380 and 780 nm. Although it corresponds to a peak in the solar spectrum, it is only a part of the radiation, and properties with regard to visible light generally cannot be extrapolated to the whole spectrum.

Solar radiation incident on a building is composed of a direct, a diffuse and a reflected component, as illustrated in Figure 1. The direct component corresponds to a straight beam from the sun to the building. The diffuse component corresponds to radiation scattered by the atmosphere in all directions. The reflected component has been reflected from non-atmospherical objects, mostly from the ground.

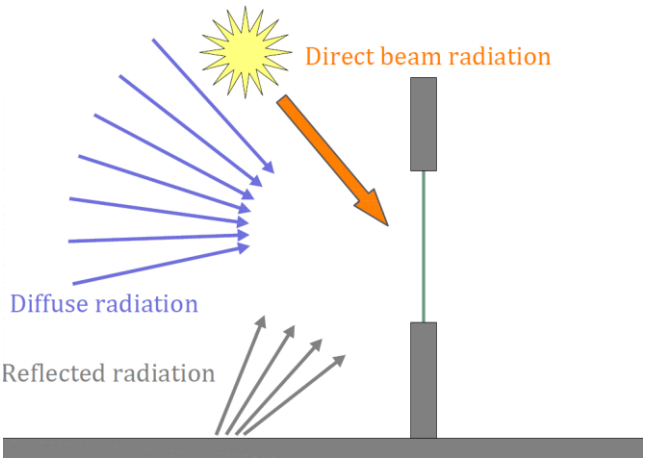

Figure 1: Direct, diffuse and reflected radiation

The determination of the properties of glass with regard to solar radiation, in a simplified way, is specified in the international standard ISO 9050. The European standard EN 410, which is refered to in the simulation software used in the following, follows a very similar approach. All parameters are determined for "quasi-parallel, almost normal radiation incidence".

In ISO 9050, the first initial parameters for a glazing layer are the spectral transmittance $\tau(\lambda)$, the spectral external reflectance $\rho_0(\lambda)$ and the spectral internal reflectance $\rho_i(\lambda)$. These are given for a wavelength range of 300 nm to 2500 nm, which includes the visible light spectrum. From these parameters, one can calculate the transmittance, external reflectance and internal reflectance of multiple glazings, for light, and for solar radiation as a whole.

An incident solar radiant flux is divided into a transmitted, a reflected and an absorbed part, which is expressed as $\tau_e + \rho_e + \alpha_e = 1$, where τ_e is the solar direct transmittance, ρ_e the solar direct reflectance and α_e is the solar direct absorptance.

The most widely used characteristic number is the total solar energy transmittance g. It indicates the total fraction of incident solar energy which is transmitted through a building component. It can be calculated as the sum of two parts: the direct solar transmittance and the secondary internal heat transfer factor. $g = \tau_e + q_i$

For double glazing, the spectral direct solar transmittance is given by equation (1).

$$\tau(\lambda) = \frac{\tau_1(\lambda)\tau_2(\lambda)}{1 - \rho'_1(\lambda)\rho_2(\lambda)} \quad (1)$$

where τ_1 and τ_2 are the respective solar transmittances of the outer and inner panes, ρ_2 the reflectance of the inner pane in the direction of incident radiation, and ρ'_1 the reflectance of the outer pane in the direction opposite to incident radiation, as illustrated in Figure 2.

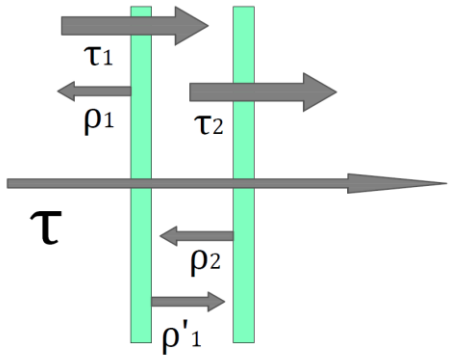

Figure 2: Illustration of the solar transmittance and reflectance properties in the case of a double glazing

ISO 9050 also gives formulae for q_i, the secondary heat transfer factor towards the inside, such as equation (2) for single glazing.

$$q_i = \alpha_e \frac{h_i}{h_e + h_i} \quad (2)$$

h_e and h_i are the heat transfer coefficients towards the outside and inside. For double glazing, the calculation is already more complicated, in that it considers the spectral characteristics for each wavelength. In

equation (3), α_{e1} and α_{e2}, respectively solar direct absorptance of the outer and of the inner pane within the double glazing, are indeed wavelength-dependent. Λ is the thermal conductance between the outer and the inner surface of the double glazing.

$$q_i = \frac{\left(\frac{\alpha_{e1} + \alpha_{e2}}{h_e} + \frac{\alpha_{e2}}{\Lambda}\right)}{\left(\frac{1}{h_e} + \frac{1}{h_i} + \frac{1}{\Lambda}\right)} \qquad (3)$$

However, tools such as EDSL Tas do not work with spectral values, but with a single value. By getting rid of the spectral dependance in the formulae from ISO 9050, one obtains the formulae in (4).

$$\alpha_{e1} = \alpha_1 + \frac{\alpha'_1 \tau_1 \rho_2}{1 - \rho'_1 \rho_2}$$
$$\alpha_{e2} = \frac{\alpha_2 \tau_1}{1 - \rho'_1 \rho_2} \qquad (4)$$

For the example of the double glazing installed in the monitored room, these formulae yield the numbers summarized in Table 18.

U-value

The thermal transmittance of a window without these solar effects can be calculated according to a second standard, ISO 10292/EN 673. The Tas Building Simulator calculates the U-value according to EN 673.

In formula (5), the thermal transmittance of a fenestration product is derived from the respective thermal transmittance of the glazing and of the frame, weighted with their respective surfaces, with the addition of a linear thermal thermittance term Ψ accounting for the interaction between frame and glazing.

$$U_t = \frac{\sum A_g U_g + \sum A_f U_f + \sum l_\Psi \Psi}{A_t} \qquad (5)$$

The glazing U-Value, U_g, depends on h_i and h_e, the external and internal heat transfer coefficients, and on the thermal conductance of the glazing itself, h_t.

$$\frac{1}{U_g} = \frac{1}{h_e} + \frac{1}{h_t} + \frac{1}{h_i} \qquad (6)$$

The thermal conductance of the glazing depends on the thermal conductance of the material layers and of each gas space between them, as expressed in formula (7), where N is the number of material layers, d_i the thickness of layer i, r_i its thermal resistivity, equal to 1.0 m.K/W for soda lime glass, and h_i the thermal conductance of gas space i.

$$\frac{1}{h_t} = \sum_{i=1}^{N-1} \frac{1}{h_i} + \sum_{i=1}^{N} d_i \, r_i \qquad (7)$$

The thermal conductance of a gas space is the sum of its radiation conductance and of its gas convection conductance. In the double glazing installed in our object room, a coated glass surface yields a lower radiation conductance as for uncoated glass. This is the principle of so-called low-emissivity glazings, as present in the monitored room presented hereafter.

Global approach

The separation of "night-time" thermal transmittance and solar transmittance, as above, although it gives insight into the thermal behaviour of glazings, is not representative of actual conditions.

Another approach consists in setting up the energy balance equations for every glazing layer, taking into account the solar absorptance and actual temperatures. This allows the calculation to model more adequately the complex energy interactions taking place in glazed areas. This approach is adopted in dynamic simulation tools such as EDSL Tas, and in the standard ISO 15099.

2.1.2 Shading devices in buildings

Solar gains increase cooling loads or, in the absence of air conditioning, can lead to overheating in the summer. To reduce excessive solar gains, one may either use solar control glass, or provide some shading. We will focus on devices that give this second possibility.

First of all, it should be reminded that the prevention of overheating is not the only purpose of shading devices. Often, shading devices aim at preventing from direct sunlight or from other light sources, at controlling glare, or at granting privacy, while preserving a certain degree of natural lighting, and a visual link to the exterior. As far as energy consumption is concerned, it makes sense to consider lighting electricity use along with cooling load reductions when predicting the energy efficiency of different window choices (Sullivan et al. 1992). Additional issues to be regarded may include airflow modification, resistance to wind and atmospheric conditions, acoustics and esthetics.

Shading devices can take many forms, and one may distinguish them with different criteria: According to their position in relation to the glazing, shading devices can be internal or external, or located between glazing layers. They can be fixed, or dynamic. Dynamic or operable shading devices can in turn be distributed according to their possible movements, including folding, gliding, drawing down, lifting up, and tilting in different directions.

The term “window blind” is ambivalent, in that it can refer generally to any window covering, or to some specific types. A blind can be defined as “something to hinder sight or keep out light” (Merriam-Webster 2013).

A frequent type of blind is the so-called Venetian blind, which features “numerous horizontal slats that may be set simultaneously at any of several angles so as to vary the amount of light admitted”. A Venetian blind can be situated either inside or outside of the window, or also integrated between the panes. As mentioned in the previous definition, this kind of blinds is characterised by the angular movement of its horizontal slats. Generally, the slats can also be lifted up when the user does not need the blind.

Another frequent movement type for window shades is to roll down on the window and roll up out of the way. In this case we speak of roller shades. These shades vary with the roller systems they are mounted on, and with the actual shading materials. These are mostly textile materials

with different opacities. Roller shutters function with the same principle, but are made out of numerous horizontal slats hinged together.This grants a certain rigidity, which makes them suitable for outside use and security applications.

Apart from roller shutters, window shutters usually refer to hinged covers for windows. These in turn are frequently fitted with louvers. A louver is a framed opening fitted with fixed or movable horizontal slats, the word being also sometimes used for one of the corresponding slats.

While all the previous devices are parallel to the window plane, usually vertical, other shading devices can reach out of this plane. Fixed shading devices of the sort include overhangs, reaching above the windows, and lateral fins. A combination of horizontal overhangs and lateral fins results in a so-called egg-crate shade. Even more than other shading systems, these protruding devices should be chosen according to the latitude and to the orientation of the building. Similar to an overhang, the awning, “a rooflike cover extending over or in front of a place”, protects from the sun and from the rain, and can be operable.

2.1.3 Effectiveness of a shading system

Various shading systems have different effects on the thermal behaviour of windows, and quantifying them requires special care. Different boundary conditions affect the effectiveness of blinds, shutters and other shading systems, among which the direction of the incident irradiation, the proportion of direct and diffuse radiation, the glazing itself, the wind conditions and the ventilation of the gaps. As as result, it has been said (Kuhn et al. 2001) that there are “no reliable standard methods for the evaluation of the effectiveness of sun-shading systems”.

Still, when trying to quantify this effectiveness, one can use the total energy transmittance g of a shaded window, as already introduced in 2.1.1 for non-shaded windows. This number can be determined either by direct measurement, or by calculation. Direct calorimetric measurements are expensive and time-consuming, but the only reliable method to validate a calculation method (Kuhn et al. 2001). The cited article also insists on the

importance of angle dependency for reliable evaluation of overheating protection, and on the necessity of considering shading systems together with an associated control strategy. Decomposing the system in layers, one can also measure layer-specific inward-flowing fractions of absorbed solar energy (Klems & Kelley, 1996) for a number of configurations of fenestrations with shading.

2.2 Dynamic building simulation

In the following, we define dynamic building simulation, first in general, then in particular with the software used in this work. We then introduce the modelling of shading systems in dynamic simulation, and the calibration of dynamic building simulation.

2.2.1 Introduction to dynamic building simulation

We define dynamic building simulation as the use of computer software to model the dynamic, time-varying behaviour of a building, in terms of energy, temperatures and other related variables. This approach is sometimes also referred to as building energy simulation or building thermal analysis. Dynamic building simulation programs can be opposed to stationary or quasi-steady-state tools, which operate on the basis of monthly or even yearly balances. One characteristic of dynamic or transient calculation methods is that the inertia of the building is taken into account to determine the temperature at each time step. On the other hand, quasi-steady-state methods substitute empirical gain utilization factors for these dynamic effects.

As calculations become more detailed, comprehending them and accounting for their validity becomes more difficult. The software used in this work is checked against different standards, among which EN ISO 13791, ASHRAE 140-1 and CIBSE TM33.

ASHRAE Standard 140, Method of Test for the Evaluation of Building Energy Analysis Computer Programs, was the first codified method of test for building energy software. Its methodological foundation (Judkoff, 2006) relates to the three ways in which the accuracy of a whole-building

energy simulation program can be evaluated: empirical validation, analytical verification, and comparative testing. These three validation techniques, each with advantages and shortcomings, are applied both to simulation of the building envelope and simulation of mechanical and on-site energy generation equipment.

ISO 13791 specifies the assumptions, boundary conditions, equations and validation tests for a calculation procedure, under transient hourly conditions, of the internal temperatures (air and operative) during warm periods, of a single room without any cooling/heating equipment in operation. ISO 13790 presents calculation methods for the energy use for the space heating and cooling of a building, at different levels of detail, the most detailed being “dynamic simulation” on an hourly basis. EN 15265 presents general criteria and validation procedures for transient calculation methods of the thermal and energy performance of buildings.

2.2.2 EDSL Tas and its calculation principles

EDSL Tas follows the approach of dynamic simulation as introduced above. According to the Theory Manual (EDSL, 2012), five different modes of heat transfer are considered: conduction, convection, advection, long-wave radiation and solar radiation. A key point in dynamic simulation is the dynamic treatment of conduction through the different layers of the building fabric. In Tas, it relies on the so-called thermal response factor method. This method was first introduced (Mitalas and Stephenson 1967) for a single room. It takes its name from the fact that it calculates the “factors influencing the thermal response” of a system constituted by the elements of the room following an excitation. In this first paper, the unknowns were temperatures and the cooling load, and the excitation a heat gain through exterior surfaces by convection and radiation.

The method takes into consideration the heat stored in walls, floor and ceiling, as well as internal heat transfers by radiation and, separately, convection. The calculation of this thermal response is based on the equations of heat balance for each of the surfaces that delimit the room,

and for the room air. The equations expressing the wall temperatures, the air temperature and the excitation of the system are written as a matrix. The solution of the problem then amounts to an inversion of the matrix. Thermal response factors (Wiese, 1982) “can be defined as time-dependent heat transfer coefficients which depict an object’s action upon a particular outside surface/inside surface temperature difference over a period of time”.

Thus, conduction is treated with the thermal response method using a one-dimensional model for opaque surfaces. For glazing, a “multi-layer conduction model with nodes” is used, and the thermal mass is neglected. The temperature of a glass layer at a given time depends only on the solution of the heat balance equations at this time, and not on its previous state.

Convection at building surfaces is treated using a combination of empirical and theoretical relationships relating convective heat flow to temperature difference and surface orientation for internal convection, and to wind speed for external convection.

Long-wave radiation exchange is modelled using the Stefan-Boltzmann law with surface emissivities coming from the materials database. Long-wave radiation from the sky and the ground is treated using empirical relationships.

Regarding solar radiation, it is distinguished between direct and diffuse solar radiation. Each Tas weather file provides hourly values for global and diffuse solar radiation measured on the horizontal. The direct radiation, which is equal to the difference between these two quantities, can be multiplied by a vector accounting for the sun position, which results in a solar beam vector pointing in the direction of the solar beam, and whose magnitude is the direct normal solar radiation flux. The direct solar radiation incident on a surface is then calculated as minus the inner product of this direct beam solar vector with the outward-pointing area vector of the surface. Where applicable, the direct incident radiation is

reduced by a shading factor resulting from shading calculations or from the effect of feature shades, as described in 2.2.3.

The diffuse solar radiation, as well as the ground-reflected radiation, is assumed to be isotropic. The diffuse solar radiant power incident on a surface is therefore a simple function of the surface tilt, independent of the sun position. It is important to note that Tas does not account for diffuse radiation shading.

Solar radiation affects both opaque and transparent constructions. The solar transmission and absorption characteristics of transparent constructions are “derived in advance of simulation from the properties of its constituent layers”. This is done by tracing of a normal ray in the construction, from both sides. The resulting normal incidence absorptances (for each direction) and transmittance can be viewed in the construction editor.

The Theory Manual (EDSL, 2012) defines advection as “the transfer of heat via the bodily movement of air”. An interesting feature of Tas is the combination of dynamic thermal simulation with natural ventilation calculations: windows, doors and other so-called apertures have their relative altitude and orientation calculated “to give a potential airflow network through the building”. Thus natural ventilation is “simulated automatically”. What is more, it can be defined when and by how much each aperture is opened.

In contrast to early applications of the thermal response factor method, Tas Engineering is not restricted to a single room, but able to treat a high number of different zones in the same building. Different zones should be applied whenever two spaces are meant for a different use, or supposed to have different temperatures.

2.2.3 Simulation of shading systems

Taking into account shading systems in a dynamic building simulation can be done in various ways. Like for glazings without shading, the emphasis often lies on the calculation of the total solar energy transmittance, or g-value, the fraction of solar energy eventually getting inside of the window system.

On the one hand, one may simply change some glazing characteristics. Most simply, a lower value accounting for the shading can be substituted to the original g-value of the glazing. Typically, the original g-value is multiplied by a so-called shading factor. For instance, in the ÖNORM B 8110-6, the Austrian standard for heating demand and cooling demand, “reduction factors” are given for different types of adjustable shading systems, and depending on the g-value of the unshaded window. For a window with a g-value of 0.70, the factors are 0.15 for external Venetian blinds and 0.70 for internal Venetian blinds. However, simulation tools like Tas do not resort to the g-value in their calculations, but dynamically to the different properties of each layer of the glazing. Also, the dependency on the incident angle is important, which has led to the replacement of the shading coefficient by the solar heat gain coefficient (SHGC), quantity with an explicit dependence of incident angle (Klems, 2002).

On the other hand, the actual geometrical shading can be calculated. This is easier for fins, overhangs and other geometrically simple shading devices. For louvered shades, the simulation has to take into account the possibility of multiple reflexions and scattering. This can be achieved, for instance, by methods of ray-tracing (Kuhn et al. 2001). For louvered shades, the goal is to characterize shading elements by their spatially averaged optical properties. A calculation speed adapted to dynamic building simulation always involves using some simplifications. An analysis of the simplifications suggested by different authors (Saelens et al. 2013) can lead to the conclusion that using monthly averages would potentially be a good compromise between calculation effort and accuracy. Usual simplifications are to make the problem two dimensional, meaning

without window edges, and to consider the slats flat and with no thickness.

Another frequent simplification is to consider that the slat reflection is only diffuse, and not specular. This is assumed in the already mentioned ISO 15099, which includes a procedure to calculate the properties of “slat type” shading devices. Considering two slats, view factors are calculated for direct-direct transmission, direct-diffuse transmission and reflection, and diffuse-diffuse transmission and reflection. Apart from the direct-direct transmission, all other factors are wavelength dependent. It is reminded that the slats are semi-transparent for infrared radiation, which also needs to be taken into account. The comparison of the properties of solar protection devices as obtained with calculations according this standard and from experimental measurement with calorimeters (Knauer et al. 2004) shows a good performance of this model, though limited when applied to more complex systems with non flat slats.

Going further, interreflexions between the slats and the glass panes can also be considered (Pfrommer et al. 1996). In addition to changes in solar radiation gains, changes in volume flow rates and air velocities can be simulated, which has been implemented for instance in EnergyPlus (Bayraktar & Ok, 2009). Internal blinds have a significant influence on convective heat transfer from windows. Experimentally, it has been shown (Clark et al. 2013) that the natural convection coefficient at a window surface with Venetian blinds is lower than without blinds, and dependent on the slat angle. Beyond energy demand, indoor air quality, daylight, and visual comfort have also been considered (Nielsen et al. 2011).

The simulation of shading systems specifically in the tool used in the following work is described in 3.2.3. It is possible to simply change physical parameters of glazings, for instance by adding a “blind layer”, as well as to calculate geometrical shading by slat type shades, overhangs and fins. Nevertheless, important simplifications are present in each case.

Material properties of shading systems

The previous calculation methods require data concerning the physical properties of material. Whichever simulation method is chosen, at least one value for solar reflectance ρ or absorptance α would be needed. For materials transparent to certain wavelengths of solar radiation, the transmittance τ is also needed. A value for long-wave emissivity is also necessary for the modeling of long-wave radiation. When relevant, bidirectional properties are needed. If calculations are separated for different wavelengths, the number of required values is accordingly multiplied.

Some values are available for fabric blinds. For instance, the company Helioscreen (Helioscreen, 2011) gives values of solar transmittance, reflectance and absorptance, as well as visual transmittance, for its "sunscreen" fabrics. One white fabric for internal use has a high solar reflectance $\rho = 0.654$ and a solar transmission $\tau = 0.229$. Another fabric for external use has a reflectance $\rho = 0.29$, a transmission $\tau = 0.14$, and an "external solar factor" of 0.12.

For louvered blinds, data from one manufacturer was found (Warema, 2013). Transmittance and reflectance are indicated for the slats on the one hand, and for the whole shading system on the other hand. In the latter case, the values are computed on the basis of standards EN 410 (CEN 1998) and EN 13362-2 (CEN 2006), for given angles of the sun elevation and of the slats, as represented in Figure 18. Some of these values are reproduced in Appendix A, in Table 19 for the slats, and in Table 20 for the whole system at given angles.

Aluminium is the mostly used material for slats. Interestingly, its properties vary greatly not only with the incident wavelength, but also with the temperature and the way it is treated. The spectral reflectivity of aluminium is mostly superior to 0.9 between 300 nm and 3000 nm, with a local minimum of 0.86 around 800 nm (Gustavsen & Berdahl, 2003). The high emissivity ($\varepsilon = 0.9$) of anodized aluminium surfaces can be contrasted (Bartl & Baranek, 2004) to the low emissivity of the metallic

surface ($\varepsilon = 0.2$, and even lower if it is polished and not oxidized). In an article dealing with the calculation of the effective solar properties of a Venetian blind layer for building energy simulation (Kotey et al. 2009) we find a slat surface reflectivity of 0.673 and a slat transmittance of zero for light colored blinds. TAS offers three default blind "materials": light, medium and dark (see Table 4). They are to be taken as spatially averaged layer properties, and not as slat material properties.

2.2.4 Calibration of dynamic building simulation

"To calibrate" means "to standardize by determining the deviation from a standard so as to ascertain the proper correction factors" and "to adjust precisely for a particular function" (Merriam-Webster, 2013). In the context of dynamic building simulation, calibrating consists in reconciling building models with measured data.

Measured data often consists in the energy use. In an illustrative article (Norford et al. 1994), calibration is used to explain a two-to-one discrepancy between measured and predicted performance of a "low-energy" office building. Interestingly, the discrepancy is mostly due to the use of the building, rather than to the construction itself. In another article, a similar approach is developed with criteria of mean bias error and root mean squared error (Pan et al. 2007).

Measured data can also be obtained from the monitoring of the building, as in this work. For spaces subject to overheating without space cooling, this seems to be the only solution. Temperature and other variables are measured at frequent intervals, so that a closer link can be established between measured and simulated data. Such an approach toward to calibration has for instance been presented for the analysis of tradidional buildings (Mahdavi et al. 2007). In particular, a weather station installed in proximity of the object is instrumental in providing the simulation with high quality empirical data. Another "approach to the calibration of building energy simulation models" (Clarke et al. 1993), applied with the

ESP-r tool and monitoring on test cells, included the analysis of residuals (difference between simulated and measured temperatures) at difference frequencies and the determination of their cause. It also presupposed the gathering of a “high quality data set”. Other ways to improve calibrated hourly simulation models (Bou Saada & Haberl, 1995) include different calibration plots, and statistical methods to evaluate the goodness-of-fit. The use of error indicators can make the calibration procedure more systematic, and even allow it to be treated as a numerical optimization (Tahmasebi et al. 2012).

In a paper applying sensitivity analysis to building simulation calibration (Westphal & Lamberts, 2005), the shading coefficient was found to be the parameter having the most influence of the cooling load of an office building. The consideration of shading in the calibration of dynamic building simulation is an intricate, but necessary task. Still, it does not seem to have been distinctly examined, apart from an empirical validation of shading algorithms in dynamic building simulation tools thanks to two test cells (Loutzenhiser et al. 2007), carried out for internal and external diffuse shading screens. If the programs were found to give accurate predictions for the cooling energy demand for long periods of time, the predictions for instantaneous cooling power were poorer.

2.3 Building monitoring

Building monitoring plays a central role in the approach of calibrated dynamic building simulation. Still, the necessary data that it provides should be taken cautiously. In the following, sensors are presented with their properties, as well as the physical principles used for the measurement of temperature, humidity and other relevant variables.

2.3.1 Sensors and their physical principles

A sensor is a device that responds to a physical stimulus and transmits a resulting impulse. Most sensors have two “components”: a transducer that transforms the measured signal into a convenient electrical signal,

and a signal conditioner. Some of the important properties of sensors are range, sensitivity, accuracy, repeatabality, and stability.

The range of a sensor gives the minimal and maximal values of the parameter that can be measured.

Sensitivity can be defined as the ratio of the resulting output change to a change of the input, or as the minimum input of physical parameter that creates a detectable output change, which is also called the resolution. The response time of a sensor is the time it takes for the output to adapt to a change of the input.

Accuracy is the maximum difference that would exist between the actual value and the indicated value at the output of the sensor. Precision, or repeatability, measures the variation of outputs that the same input will produce under identical conditions.

Stability describes the ability of a sensor to keep the same properties over time. Drift occurs when these properties are subject to a slow degradation in time.

The main categories of temperature sensors are thermocouples, thermistors and resistance temperature detectors (RTDs). Thermocouples are advantageous for temperatures above 200 °C. Thermistors, made from certain metal oxides whose resistance decreases with increasing temperature, are usually economical, but less accurate and stable than RTD's. These are made of metals such as platinum or nickel whose resistance increases with temperature.

The most accurate humidity sensors are chilled mirror dewpoint hygrometers. Other electronic hygrometer types are capacitive, resistive and thermal conductivity humidity sensors.

NDIR "non dispersive InfraRed (NDIR)" sensors are the most frequently used to measure concentrations of carbon dioxide, based on the absorption of a characteristic infrared wavelength by this gas. Their long-term stability is particularly problematic.

In calibrating dynamic building simulation, one should not forget that the measuring tools themselves need to be calibrated.

2.3.2 Building monitoring systems

Temperature, humidity and concentration of carbon dioxyde being some of the most important parameters of the inside environment, the above-mentioned sensors can be deployed in buildings for monitoring. Usually, sensors are incorporated in data loggers of reduced size, which can be fixed on walls or at other defined locations. The number of sensors and their placement in the building depend on the intended use of the monitoring, and are the result of a compromise between costs, energy use, and accuracy. The expected distribution of air temperature in the room should also play a role.

The installation location of temperature sensors should be chosen in order to avoid interfering thermal phenomena (Klaassen, 2001). These include solar radiation from windows, cooling sources, heating sources, and office equipment.

Solutions using energy harvesting now make the deployment of sensors without batteries and wires possible. This is the principle of the EnOcean technology, applied in some of the measuring devices used in the following.

Chapter 3

Methodology

Monitoring takes place in an office room in Vienna, Austria. First, available data and reasonable assumptions are used to simulate the room with a dynamic building simulation tool, EDSL Tas, Version 9.2.1.5. Different shading systems are then applied to the simulation, and their effects are compared. This leads to the choice of two shading systems: external and internal Venetian blinds. The monitoring of the room, successively without shading, with internal and with external shading, is then used to calibrate the simulation in several steps.

3.1 Test case

The object of our monitoring and simulation is a room situated in the main building of the Vienna University of Technology at Karlsplatz, in the fourth district of Vienna. The climate in Vienna is characterized by both oceanic and continental influences. Although it can be described as a heating-dominated climate, summer overheating can be an issue. The average high temperatures in June, July and August vary between 22 and 26 °C.

3.1.1 Room description

The object room is situated on the top floor of the middle wing the main building of the Vienna University of Technology. This middle wing was first built from 1836 to 1839, but the third and fourth storeys were added from 1867, and the top floor in the 20th century. The room (1 in Figure 3) has a relatively high proportion of surfaces exposed to the exterior. It is to be used as an office room, with a capacity of three work stations.

Adjacent rooms are a staircase (4 in Figure 3) and an unheated “tower” (2 in Figure 3) that reaches several floors higher, as well as a small server cabinet (3 in Figure 3). The tower is almost not occupied, apart from people accessing the

weather station. Under the room is a low unused interval space, and underneath usual university rooms.

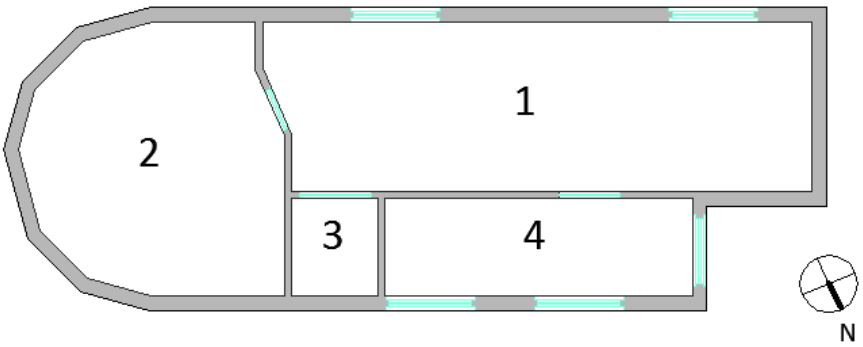

Figure 3: Floor plan. 1: object room, 2: tower, 3: electric compartment, 4: staircase.

Windows

The main external wall, oriented south-southwest, is equipped with two identical windows. This orientation makes the room prone to overheating.

The frame is a wooden frame made out of spruce. The reference of the glazing is “SGG Climaplus Ultra N”. It is a double glazing with a 16 mm argon-filled cavity.

The glass panes both measure 4 mm. One of them is a low emissivity glass: “Sgg Planitherm Ultra N”. It is coated on the cavity side in order to have a low thermal emissivity. Since the climate is heating dominated, we assume this low emissivity pane is the one on the room side, which means that surface number 3 in Figure 4 is coated. The coated surface could also be surface number 2. This would make a difference, as discussed in 4.1.

According to the manufacturer, this glazing has a U-Value of 1.1 W/m.K (after EN 673). The g-value (after EN 410) is equal to 0.63 with the coating on surface 3, and equal to 0.58 with the coating of surface 2.

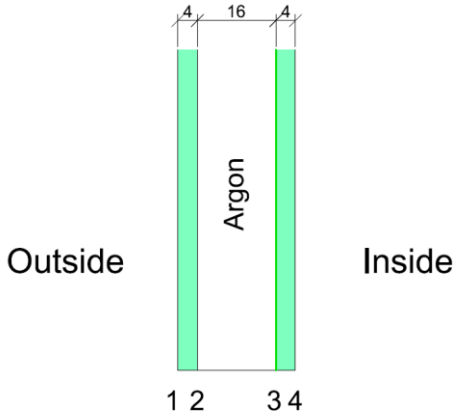

Figure 4: Double glazing section

3.2 Simulation of the room

In the following, we describe how the previously described object is represented in the dynamic building simulation tool, EDSL Tas, from the modelling to its calibration, and including different shading systems.

3.2.1 Modeling of the room

The simulation of the room begins with its modeling in the TAS 3d Modeller. A building is divided in different floors, to be defined with the corresponding heights. The piece of software allows the user to view the model in three dimensions, or in two dimensions for every floor.

On a given floor, the first elements to be defined are wall surfaces. Walls then define spaces, to which floor and ceiling/roof elements can be attributed. Each of these surfaces has a given building element attributed to it, whose properties at this stage are its width and its transparent or opaque character. In a similar way, spaces can have zones attached to them. If no zone is attributed to a space (<None> zone), the boundaries between this space and other “zoned” spaces are then considered adiabatic.

Further, window (or door) instances can be added to existing walls, once window elements have been defined, with the corresponding width, height, level and frame width.

Once the 3d model is complete, it can be exported to the Tas Building Simulator. This “analysis” of the building geometry can include or not shading calculations. These calculations being quite time consuming, they can also be carried out only for given days of the year, with a given frequency.

In the Tas Building Simulator, “constructions” are affected to the previously defined building elements. These constructions are stored in a separate constructions database.

For the building elements surrounding the studied room, the constructions in Table 1 were defined. The layer composition is based on probable assumptions, and the total thickness of each element is measured approximately. The featured U-Values correspond to the outputs readable in Tas, for the flow direction in which each construction will be used, and rounded to two decimals.

Each layer corresponds to a certain material. Materials are also regrouped in a “materials database”. The materials used for the constructions defined in Table 1 are given in Table 2, with their respective thermal conductivities, densities and vapour diffusion factors μ. In addition to these characteristic values, the specific heat (in J/kg.K), the solar reflectance, the light reflectance and the emissivity, are also listed for each material.

Table 1: Constructions

Construction	Layer	Thickness (cm)	U-Value (W/m.K)
External wall		32.0	1.50
	Internal plaster	1.0	
	Masonry	30.0	
	Exterior rendering	1.0	
Internal wall 1		18.0	1.80
	Internal plaster	1.0	
	Masonry	16.0	
	Internal plaster	1.0	
Internal wall 2		47.0	0.86
	Internal plaster	1.0	
	Masonry	45.0	
	Internal plaster	1.0	
Internal wall 3		36.0	0.99
	Internal plaster	1.0	
	Masonry	35.0	
	Internal plaster	1.0	
Ceiling		26.5	1.09
	Internal plaster	1.0	
	Lightweight panel	5.0	
	Reinforced concrete	20.0	
	Roof sheet	0.5	
Floor		34.2	1.36
	Parquet flooring	2.20	
	Screed	6.0	
	Sand	14.0	
	Concrete slab	12.0	
Door entrance		5.5	0.83
	Steel layer	0.5	
	Insulation	4.5	
	Steel layer	0.5	
Door tower		4.0	1.83
	Wood	4.0	
Door closet		0.15	3.85
	Metal sheet	0.15	

Table 2: Assumed construction materials

Layer	Material	Conductivity (W/m.K)	Density (kg/m³)	μ (1)
Internal plaster	Gypsum-lime	0.50	1300	11
External rendering	Cement	1.15	1600	22
Masonry	Brick	0.70	1700	8
Lightweight panel	Wood wool	0.10	465	15
Concrete ceilling	Concrete	1.83	2400	24
Roof sheet	Aluminium	204.00	2700	99999
Parquet flooring	Softwood	0.14	500	12
Screed	Concrete	1.28	2100	34
Fill	Sand and gravel	1.30	2240	34
Slab	Concrete	1.40	2360	34

3.2.2 Calibration of the model

Before attempting to calibrate the simulation model, it is important to remind all the possible sources of errors. It can be distinguished between “internal” and “external” errors (Judkoff, 2006). We assume that internal errors are negligible, the used software being tested and recognized, as seen in 2.2.1 (Introduction to dynamic building simulation). We are then left with external errors, which can be grouped as follows, as in the mentioned article:

- Differences between the actual microclimate that affects the building versus weather input used by the program. Given the use of data from a very close weather station, these differences should be minimal.
- Differences between actual schedules, control strategies, effects of occupant behavior, and other effects from the real building versus those assumed by the program user.
- User error in deriving building input files.
- Differences between the actual physical properties of the building (including HVAC systems), versus those input by the user.

Sources of external errors are potentially all variables input in the simulation tool. This corresponds to the different parts of the tool that are successively used.

Three-dimensional model

This begins with the geometry of the simulated building. Inaccuracies in the geometry input in the Tas 3d Modeler are unavoidable, but limited to a few centimeters for the length of each wall. An important issue is that of the limits of the model, and of its division in zones. Given the relatively high degree of exposition of the room on the last floor, it is not necessary to model the whole building to get a good approximation of the thermal behaviour of the room. Still, it makes sense to include adjacent rooms. It was decided to consider three zones: the office room itself, the the staircase next to it, as well as the “tower”. Since heights are determined for each floor, both three have the same height in the model. In the case of the tower, which is much higher, this does not correspond to reality, but results show that this approximation does not prevent simulated temperatures to fit measured temperatures quite well. In the calibration process, a fourth zone is added, corresponding to the lower part of the staircase.

Building environment

After the export of the 3d model to the Tas Building Simulator, one gets to define parameters linked to the surroundings of the building, in the building summary: ground solar reflectance, building height adjustment factor, mean height of surroundings and terrain type. Apart from the ground solar reflectance, which determines the amount of reflected radiation, these parameters are used for wind pressure calculations. Additionally, a wind pressure coefficient file can be imported. The Infiltration coefficient in the heating plantroom controls tab provides a facility for making fresh air infiltration dependent on wind speed.

Building elements

The different constructions and their thermal properties are a source of uncertainty, since the assumptions are mainly based on visual inspection and on the period of construction. The way windows and doors are opened (aperture types) and shaded is also to be defined, possibly according to a schedule.

Internal conditions

The internal conditions window is organized around four tabs: internal gains, heating and cooling emitter, and thermostat. We should distinguish the monitoring and the calibration from the expected future use of the room and the prospective use of simulation.

For the measurements and the calibration, which take place in the summer period, without heating and cooling, only the first tab matters. These “internal gains” include occupancy, equipment and lighting gains, as well as infiltration and ventilation.

The room is equipped with a dimmable luminaire with three lamps and a maximal power of 100W. During the monitoring period, artificial lighting is not used in the room, but only in the adjacent staircase.

During the monitoring period, it can be said that the room was mostly not occupied to its full capacity, to such an extent that the calibration was started with a null occupancy gain.

The average metabolic rate per unit of skin area for a writing person is 60 W (ASHRAE, 2009), or 108 W for a body surface area of 1.8 m². The proportion of sensible and latent gains depends on the temperature. We can assume 70 W sensible and 38 W latent gains. Typical heat gains from the literature (Duška et al. 2007) are 50 W for a large LCD monitor and 110 W for a PC without monitor (145 W for a conservative value).

Given the nett floor area of the room (17.46 m²), we can compare values for a certain number of persons and pieces of equipment to standard values. For instance, the Austrian standard ÖNORM B 8110-5 specifies internal gains of 3.75 W per square meter of gross floor area, which can be converted to 4.85 W/m² (nett area) and distributed in different gain types to yield the figures in Table 3.

Infiltration is an important parameter, and fairly difficult to precisely estimate. A (too high) value of 0.6 ach for the infiltration rate was first assumed at the beginning of the calibration process, for all three zones.

Table 3: Assumptions for internal gains

Gain	1 person	1 person (per m²)	B 8110-5 (per m²)
Occupancy sensible gain	70 W	4.01 W/m²	1.50 W/m²
Occupancy latent gain	38 W	2.18 W/m²	0.75 W/m²
Equipment gain	160 W	9.16 W/m²	1.60 W/m²
Lighting gain	0.00 W	0.00 W/m²	1.00 W/m²
Total heat gains	268 W	15.35 W/m²	4.85 W/m²

A finer calibration of the model can be achieved thanks to the monitoring of window opening and occupancy. This represents the second step of calibration, the results of which are discussed in 4.3 (Calibration of the unshaded room). We obtain hourly values of the occupancy sensible and latent heat gains by multiplying hourly values of the occupancy (the mean of the values from the two sensors) by some gain coefficients $g^{sensible}$ and g^{latent}.

We proceed in a similar way to derive hourly values of the opening of each window from the monitored window contact values, which are equal to 1 if the window is closed, and null if it is open. However, this does not tell how wide the window is open, or if it is tilted or turned, so a coefficient k is needed, with the signification of a mean opening, so that for instance the opening of the right window is given by formula (8).

$$a^{right}(t) = k \times (1 - \frac{con_1(t) + con_2(t)}{2}) \qquad (8)$$

However, this kind of calibration is possible only for the office room itself, and not for the two adjacent zones.

Weather data

TAS uses weather data for a whole year. This data consists in hourly values for global and diffuse radiation (W/m²), cloud cover (from 0 to 1), dry bulb temperature (°C), relative humidity (%), wind speed (m/s), and wind direction (degrees).

A weather station situated only several meters away from the test room provides measurements for all these quantities except cloud cover. The cloud cover coefficient is obtained thanks to the meteonorm software. It uses an empirical formula based on the quotient of diffuse and global radiation, which can be compared to what it would theoretically be for a clear sky (Remund et al. 2013).

The first simulations analysing the effects of different shading systems are carried out with recorded data from the year 2011. In that year, the warmest day was August 26th, with a maximal outside air temperature of 35.3 °C. Using recorded data allows us to consider such peaks, which would not appear in averaged data. For calibration and all resulting simulations, weather data from the current year (2013) is used.

Existing shading

A certain degree of shading is already provided by surrounding buildings and by the building itself. Given the height of the room, the horizon is relatively free and surrounding buildings propably have a very small influence. On the other hand, the exterior wall itself, which juts out on the window sides, and the extremity of the roof construction, including eavestrough, do provide some shading. This is considered in the calibration process.

Calibration plots

Comparing the simulated temperature to the monitored temperature can be done visually, for instance by plotting both these temperatures, and/or their difference, simultaneously with weather data, and for different time intervals. Point clouds involving the difference between simulated and monitored temperature can help identify error patterns.

Error indicators

Additionally, different numerical indicators may facilitate comparisons, and offer an evaluation of the goodness-of-fit of the model.

The simplest - and very limited - indicator might be the mean difference between simulated and monitored temperatures, which is also the difference between the average simulated temperature and the average monitored temperature (9).

$$\overline{\theta^s - \theta^m} = \frac{1}{n}\sum_{i=1}^{n}(\theta_i^s - \theta_i^m) = \overline{\theta^s} - \overline{\theta^m} \quad (9)$$

Another possible indicator is the maximal value of the difference between simulated and monitored temperature, of the error. To have a better understanding of the distance between the two series, we can use the mean squared error, and its square root (10).

$$RMSE = \sqrt{\frac{1}{n}\sum_{i=1}^{n}(\theta_i^s - \theta_i^m)^2} \quad (10)$$

This root mean squared error is null if and only if the simulated temperature is equal to the average temperature at each time step. This criterion is used in several of the works mentioned in 2.2.4.

Another interesting indicator is the standard deviation of the temperature difference, which is a measure of how far the temperature difference lies from its mean (11).

$$\sigma(\theta^s - \theta^m) = \sqrt{\frac{1}{n-1}\sum_{i=1}^{n}\left((\theta_i^s - \theta_i^m) - \overline{(\theta^s - \theta^m)}\right)^2} \quad (11)$$

This standard deviation of the temperature difference is null if and only if the simulated temperature and the measured temperature differ by a constant. The mean squared error is related to the standard deviation of the temperature difference, as expressed in equation (12).

$$RMSE^2 = \frac{n-1}{n}(\sigma(\theta^s - \theta^m))^2 + (\overline{\theta^s - \theta^m})^2 \quad (12)$$

3.2.3 Simulation of shading systems in TAS

Tas offers three different possibilities for the modeling of shading systems.

3d shades

"3d shades" can be added in a similar way to that of windows in the 3d Modeller, but with a distinct procedure. Shades cannot be applied directly to the walls. They

must be applied to a <null> wall, which forms part of an external area connected to the building, as illustrated in Figure 5.

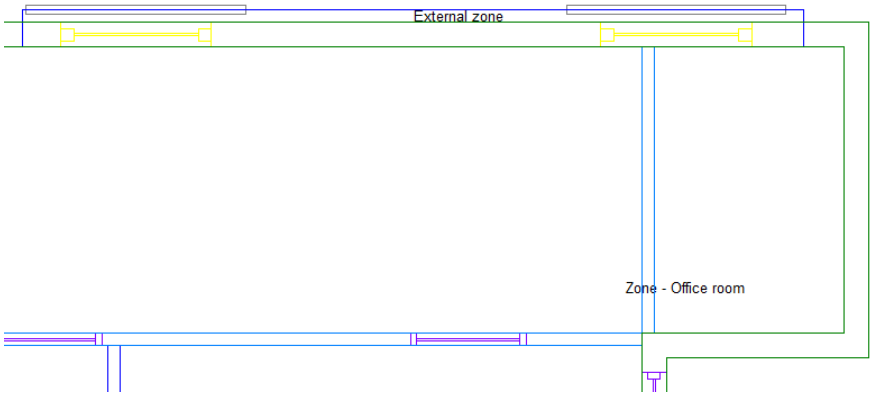

Figure 5: Plan view of "3d shades" applied 10 cm from the wall, in front of two windows

The modelled systems are only external louvered shades, as well as their frames.

Feature shades

"Feature shades" can be attributed to windows, and managed like substitute elements. With them, simple external shading types are defined in terms of side-fins and overhangs. A shading type may be assigned to any building element, and applies to all exposed surfaces of that building element type. The shading effect is combined with any shadow calculations that are performed when exiting from the 3D Modeller. The input parameters are:

- Dimensions of the shaded surface. The window is 1.24 by 1.485 m. We input a shaded surface of 1.24 by 1.485 m.
- Respectively depth, offset and transmittance, for left fin, right fin, and overhang.

Feature shades, like 3d shades, apply only to direct solar radiation. The only way to apply shading also to diffuse radiation is to modify the glazing element itself.

Substitute elements

"Substitute elements" defined in the Tas building simulator can replace given building elements according to schedules. The only requirement is that the thermal mass of the main building element and of the substitute should be negligible. This is always the case for transparent constructions in Tas. An

alternation of glass layers and gas layers has to be respected. Also, only one level of substitution is possible.

According to the software manual (EDSL, 2012), Tas accounts for the air circulation around and through blinds with a modification of the convection coefficient for gas layers adjacent to them. For a gas layer between external blinds and glazing, the convection coefficient is set to a high value of 50 W/m^2K. For a blind between glass panes, the convection coefficients for both gas layers surrounding it are increased by a factor 4/3. For internal blinds, the convection coefficient of the air layer between blinds and glazing is also increased by a factor 4/3. Still, this layer between room air and internal blinds significantly lowers the thermal transmittance of the window element.

3.2.4 Comparison of four shading systems

We simulate four different shading systems as produced by the leading German manufacturer Warema. These four systems are illustrated in Figure 6.

Figure 6: The four simulated systems. From left to right: internal venetian blind, external venetian blind, roller shutter curtain and awning. Source: Warema 2013

Internal venetian blind

The chosen model (4.50.05, sketched in Figure 7) is an internal venetian blind with cord operation. Raising and lowering the blind is done with a cord, as well as tilting the slats. A slat width of 50 mm is chosen (25 and 35 mm are also available). The top rail measures 40x36 mm. The dimensions, 1485x1240 mm,

would comply with the minimal width, maximal width, maximal height and maximal area.

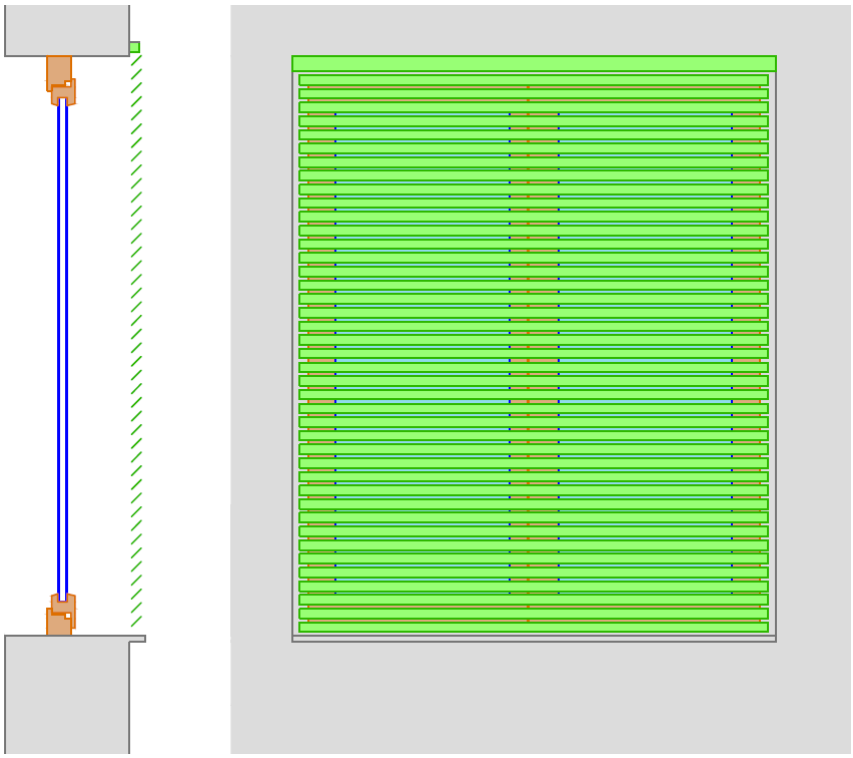

Figure 7: Window with interior blinds, in green. Left: section. Right: inside view

In TAS, the simulation of this internal blind can only be achieved with the use of a substitute element for the window construction. We obtain this substitute element using three different methods, detailed hereafter.

In the first method, one layer of air and one layer of “blind material” are added to the three original layers (glazing, argon and glazing) of the window, on their interior side, as illustrated on the left side of Figure 8.

An important parameter when simulating these internal blinds is the position of the low emissivity coating in the double glazing, as previously defined in Figure 4.

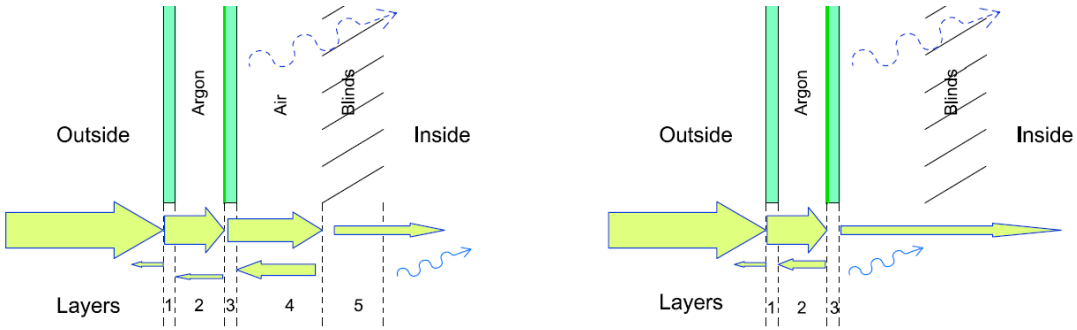

Figure 8: Layers of the window with internal blinds. Left: method 1. Right: methods 2 and 3. The yellow arrows represent solar radiation, and the ondulating lines convection. In both cases, convection through the blinds (dotted ondulating line) is not modelled

Method 2 and 3 are meant to avoid an excessive lowering of the thermal transmittance of windows through the presence of an air layer between blinds and glazing. Therefore, the interior glass layer is replaced with another single layer whose physical properties take into account both glass and internal blinds, as illustrated in Figure 8 on the right. In method 2, we tune these properties in such a way that the direct transmittance, the direct reflectance and the total transmittance of the new construction are as close as possible to those obtained with method 1.

Alternatively (method 3), we can attempt to directly calculate the properties of the layer "interior pane+blinds", by analogy with a double glazing. We resort to formulae (13) and (14), which are found for instance in the previously discussed standard ISO 9050, for direct transmission and direct reflectance.

$$\tau = \frac{\tau_1 \tau_2}{1 - \rho'_1 \rho_2} \qquad (13)$$

$$\rho = \rho_1 + \frac{{\tau_1}^2 \times \rho_2}{1 - \rho'_1 \rho_2} \qquad (14)$$

For both three methods, unsatisfactory results were obtained for certain values of the absorptance of the inside blind layer, with this layer reaching unrealistically high temperatures. The fact that dark indoor blinds can increase the peak cooling load has been mentioned in a published article (Lomanowski & Wright, 2007), with the following explanation: the solar radiation absorbed by these blinds is

"readily converted into radiative and convective energy", without the delay that is present when the same energy is absorbed by constructions with a certain thermal mass. Still, in usual cases, the decrease in solar gains should be greater than the increase in convective and radiative secondary gains, and lead to lower room temperatures.

Eventually, we consider the absorptance of the blind layer to be null, so that solar energy reaching the internal blinds is either reflected or directly transmitted. This is a simplification which prevents inappropriate results from occurring. Following this assumption, Table 4 shows the dependence of the shaded window solar properties on the blind reflectance. For the comparison with other shading systems, we use method 1, with the material properties defined as IB60 in Table 4.

Table 4: Solar properties of the internal blind layer. From left to right: very light, light, medium and dark blinds.

Window properties	No blind	IB50	IB60	IB70	IB80
Blind reflectance	-	0.50	0.60	0.70	0.80
Direct solar transmittance	0.53	0.31	0.25	0.20	0.13
Solar reflectance	0.24	0.41	0.45	0.49	0.54
Solar absorptance	0.22	0.28	0.30	0.31	0.33
g-value	0.63	0.42	0.37	0.32	0.27

External venetial blind

The second shading system is an external venetian blind with flat slats. It can be driven by a motor or by a crank, and is available with rail or cable guidance. A slat width of 80 mm is chosen (60 and 100 mm are also available). The system is attached against the wall, outside of the window recess, as illustrated in Figure 9.

The whole system, cover panel and bottom rail included, measures 1460 by 1640 mm. This agrees with the indicated minimal width, maximal width, maximal height and maximal area.

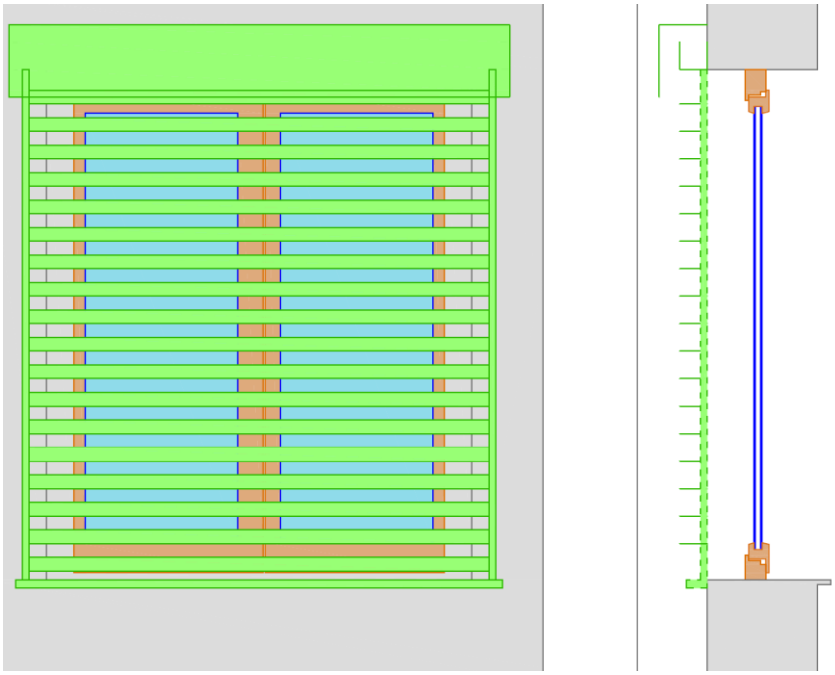

Figure 9: Window with exterior blinds, in green. Left: outside view. Right: section.

TAS offers two different possibilities to model this system. Either we can use a substitute element, like with internal blinds, or we can add the shades directly in the 3d modeller, as illustrated in Figure 10.

The advantage of the first method is that it is possible to schedule the substitute element, and that no additional shading calculations are needed. Still, it requires a correct definition of the physical properties of the "blind layer", and it does not account for the angle dependency. What is more, the problems previously mentioned for the simulation of internal blinds apply also here. On the other hand, modelling the shades in 3d yields information on the angle-dependant shading they provide at different times of the year. But it adds significantly to the computation time, and does not give the possibility of scheduling the shading.

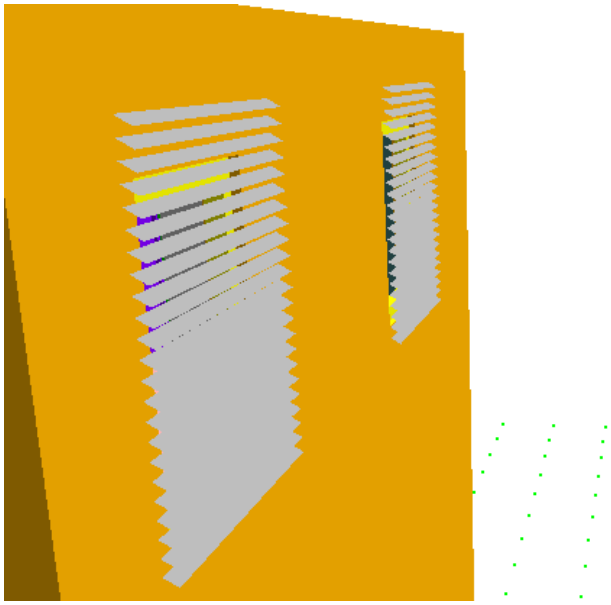

Figure 10: 3d view of 3d shades in the Tas 3d Modeller

When modelling the shades in three dimensions, the following variables have to be taken into account:

- The distance from the shade to the exterior wall. It cannot be drawn inferior to 10 cm.
- The breath and the height of the shade, which can cover a greater surface than the window.
- The number of fins or, equivalently, the vertical spacing between fins.
- The depth of the fins. Given the chosen model, this is 80 mm.
- The angle of the fins in relation to the horizontal. In Tas, a positive value means the fin plane goes upwards towards the outside, so that negative angles correspond to the interesting inclinations of the fins.
- The fin material. Only the radiative properties have an influence on the result: external and internal emissivity, external and internal solar absorptance.
- Optionally, the presence of a frame (left and right and/or top and bottom) and of vertical fins, and their dimensions.

External blinds were tested for different materials, numbers of fins and fin angles.

For the first comparison between shading devices, the blinds were modelled in three dimensions, with 31 fins (fin spacing 5.5 cm) tilted at an angle of -30 degrees (close to the optimal), made out of aluminium (see properties Refl 90 in Table 8).

For calibration and calibrated simulation, the external blinds were simulated with the second method, allowing a schedule to be applied, with the layer properties of Table 5.

Table 5: Properties of the external blind layer for three cases

Property of the blind layer	EB 30-50	EB 15-30	EB 15-50
Width	80 mm	80 mm	80 mm
Solar transmittance	0.30	0.15	0.15
Solar reflectance	0.50	0.30	0.50
Emissivity	0.85	0.85	0.85

Roller shutter curtain

The third shading system is a plastic roller shutter curtain, front-monted (V4). The height of a shutter (model K36) is 35.4 mm, and the profile thickness 8.9 mm. The maximal width, maximal height and maximal area are respected.

This system can also be modelled in two ways: with a substitute element, or with a feature shade.

In the case of a substitute element, two layers are added to the window, one of air and one of a material that is created with the assumed physical properties of the roller shutter (Table 9). Thus, the roller shutter can only be considered as drawn all the way down or all the way up. Transparent and opaque materials cannot be combined, so the roller shutter is a made of a “transparent” material, even if its light transmittance is assumed to be null.

With a feature shade of null depth, a roller shutter can be modelled in any intermediary position. For the comparison, the roller shutters were modelled as a feature shade with a transmittance of 10%, drawn 50 cm down.

Awnings

The last shading system is a drop-arm awning of type 350. The drop-arm fixation works is assured by high-tensile extruded and cast aluminium components, with gas pressure spring. The maximal arm length is 160 cm. The inclination angle of

the arm can vary from 0 to 135°. There is a wide choice of fabrics, to choose from acrylic, Soltis (technical textiles) and screen fabrics.

This system can be modelled with a "feature shade", more precisely with an overhang. Different cases are set in Table 10.

The parameter "offset of the overhang" corresponds to the vertical offset of the overhang from the top edge of the shaded surface, with a negative value for an awning. For the comparison, case 1 of Table 10 was chosen: a transmittance of 30% was assumed, and a drop-arm angle of 45%, as in Figure 11, middle.

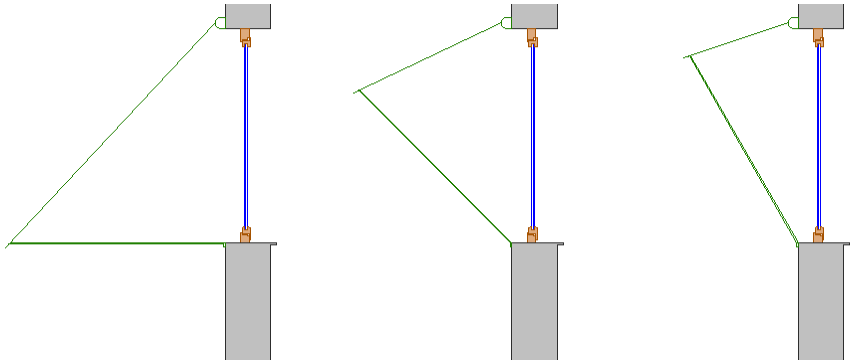

Figure 11: Section views of the drop-arm awning with arm angles of respectively 90°, 45° and 0°.

Comparison methodology

For each of the shading systems introduced above, simulations were carried out with different parameters, and one representative set of parameters was adopted for each shading system. These parameters were chosen to reflect the assumed characteristics of the systems, and in a way that allowed for meaningful comparison between them.

Since the external blinds as input in the 3d Modeller are fixed, the comparison was done for shading systems fixed over the whole season. This assumption is of course unrealistic, but it is acceptable for the comparison of cooling loads and overheating behaviour for the warm season. Calculations are carried out for the period from 1st June to 31st August.

Also, the following conditions were applied for all simulations: the internal gains were assumed to be equal to 4.85 W/m² on working hours, from 09:00 to 17:00, null otherwise. The infiltration rate was fixed to a constant of 1.0 ach.

For cooling calculations, the set-point was assumed to be 24°C on working hours, and otherwise 28°C. For overheating, the reference temperature is 27°C.

Overheating

Since we focus on overheating as a negative criterion, we can also try to observe the impact of shading not on energy transfers, but directly on the resulting degree of overheating.

To quantify the degree of overheating in an office room, we define the mean overheating in equation (15) as the sum on working hours of the differences between the inside air temperature and a reference temperature, when this difference is positive, divided by the number of these working hours.

$$OH_m = \frac{1}{n}\sum_{i=1}^{n} |\theta_i - \theta_r|_{\theta_i > \theta_r} \qquad (15)$$

As a reference temperature, we take $\theta_r = 27\ °C$.

3.3 Monitoring of the room

The room was monitored with the help of wireless sensors recording air temperature, relative humidity, CO2 levels, window positions, brightness and movements. These devices were integrated in a monitoring system sketched in 3.3.2, making possible the collection of data for different periods.

3.3.1 Measuring devices

The room was equipped with different sensors manufactured by the German company Thermokon:

SR04 CO2

The SR04 CO2 measures CO2, air temperature and humidity. The NDIR technology is used for the CO2 measurement, with automatic self-calibration. It has

measuring range of 0 to 2550 ppm for CO2, 0 to 51 °C for temperature, and 0 to 100% for relative humidity.

The typical accuracy for CO2 amounts to ± 40 ppm plus 4% of the reading. There is also temperature dependence, inferior to 0.2% per K. The typical accuracy for temperature amounts to ± 1 K. The accuracy for relative humidity at 21°C is ±3 % between 20 and 80% rH.

A self-calibration feature called ABCLogic™ is designed to correct all sensor drift, by calculating the lowest CO2 concentration taking place every 24 hours, which is assumed to correspond to outside levels of CO2.

SR04 rH

The SR04 rH measures air temperature and humidity. For relative humidity, the range is from 0 to 100 %rH, with a resolution of 0.4%rH, and an absolute accuracy of ±3% between 30% and 80%rH. For temperature, the range is from 0°C to 40°C, with a resolution of 0,15K and a typical absolute accuracy of ±0,4K.

SR65 TF

The SR65 TF is a cable temperature sensor. It has a measuring range of -20°C to +60 °C. The resolution is 0.31 K, and the absolute accuracy typically ±0.8K.

SR MDS Solar

The SR MDS Solar is an occupancy detector. It combines movement detection with a passive infrared technology, and brightness detection, with a range of 0 up to 512 Lux.

These three sensors function with the EnOcean technology (Dolphin platform). Their transmitting frequency is 868.3 MHz.

HOBO U12

Additionally, we also used HOBO U12 data loggers. These are not linked to a monitoring system, but managed manually, with a direct USB interface. They measure temperature, relative humidity and light intensity.

The range for temperature measurement is from -20 to 70°C, with an accuracy of ±0.35K between 0 and 50°C. The range for relative humidity is from 5 to 95%rH, with an accuracy of of ±2.5%rH from 10 to 90%rH.

3.3.2 Monitoring system

The monitoring system is composed of the previously mentioned sensors, of a gateway which receives data from the sensors, and of a database in which the data is then stored. One can then access the data via the local network or internet, as illustrated in Figure 12.

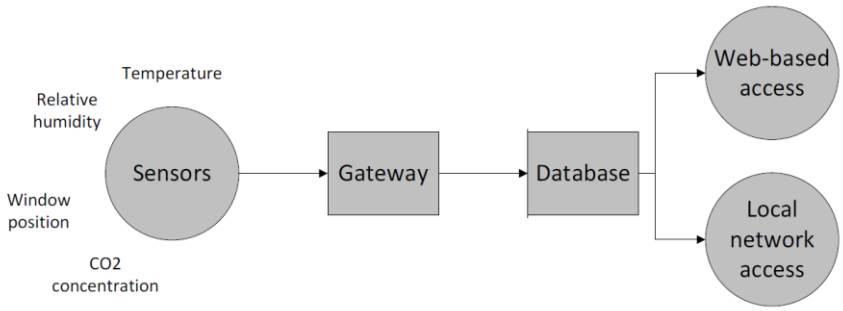

Figure 12: Principle of the monitoring system

Sensors are located in the three zones introduced in 0 (Methodology – simulation of the room): the main office room, the tower, and the staircase. Their positions are recapitulated in Figure 13 and Table 6.

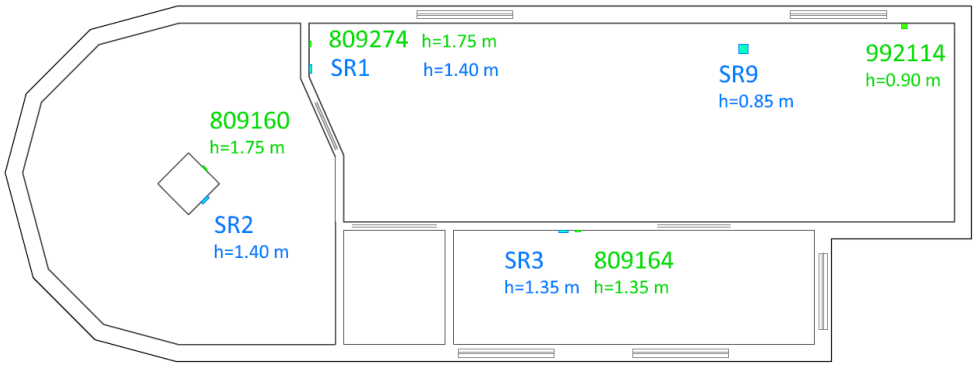

Figure 13: Position of the sensors

Additionally, contact sensors are present on each wing of the two windows of the main room. There are also two occupancy sensors, at two different locations in the room.

Table 6: List of sensors

Sensor name	Sensor type	Zone
992114	HOBO temp/rH	Office room
809274	HOBO temp	Office room
809160	HOBO temp/rH	Tower
809164	HOBO temp/rH	Staircase
SR1	SR04 rH	Office room
SR2	SR04 rH	Tower
SR3	SR04 rH	Staircase
SR4	SR04 CO2	Office room

3.3.3 Measurement periods

Measurements are carried out with different situations of the room. In a first period, the room is monitored without any shading system. Then, internal blinds are installed. Eventually, internal blinds are replaced by external blinds. These three measurement periods are listed in Table 7.

The monitoring started on 7th June at 09:00 for the four HOBO sensors. It went on continuously until 1st October, except for an interruption for the sensor 809164 on 10-11th June. The data was read out at least every three weeks. The Hobo sensors are set on local time, UTC+02:00. They record a data point every five minutes.

The weather station and the Thermokon sensors are set on UTC+01:00. The monitoring system with these sensors functioned from 12th June, with an interruption from 19th July 15:00 to 23rd July 16:00. Data points are not recorded at a regular interval, but every time a change in the measured value is registered. The resulting data is then assessed to produce hourly values.

Table 7: Measurement periods

Shading	First day	Last day
No shading	12th June	19th August
Interior blinds	20th August	11th September
Exterior blinds	19th September	28th September

Chapter 4

Results and discussion

The results are discussed following the sequence presented in the methodology, beginning with the results of the simulation of shading systems before calibration, followed by the monitoring, and the calibration, first without and then with shading devices. Eventually, the calibrated simulation is used to conclude on the effects of Venetian blinds.

4.1 Simulation of shading systems before calibration

The different shading systems were simulated and compared according to the methodology developed in 3.2.4 (Methodology – comparison of four shading systems). In the following, the results for each device are first presented, and then the results of the comparison. As a general rule, we can say that the chosen internal conditions and window opening controls contribute to relatively low cooling energy demands.

Results for internal blinds

As explained in the methodology, internal blinds are simulated by changing the building element corresponding to the windows. It has been tried to change this building element according to three different methods. Eventually, we apply the first method (as defined in 3.2.4), and we simulate the internal blinds by adding an air layer and a blind layer on the room side of the window construction. The absorptance of the blind layer is assumed to be null, to avoid unrealistically high blind layer temperatures. This yields the window solar properties already presented in Table 4.

Figure 14 and Figure 15 show the differences in simulated indoor temperatures with various internal blinds, respectively for three warm days of 2013, and for a

synthetic day resulting from the averaging of temperatures on the three-month period between 1st June and 31st August 2013. In both cases, the internal blinds lead to a lowering of internal temperatures. Understandably, the temperature difference is minimal in the morning, just before the blinds start having an effect, and reaches a maximum in the afternoon, around the time when solar radiation is maximal.

The internal blinds with a higher reflectance (0.70) and a lower transmittance do yield lower temperatures than the ones with a lower reflectance (0.50), but the difference is small.

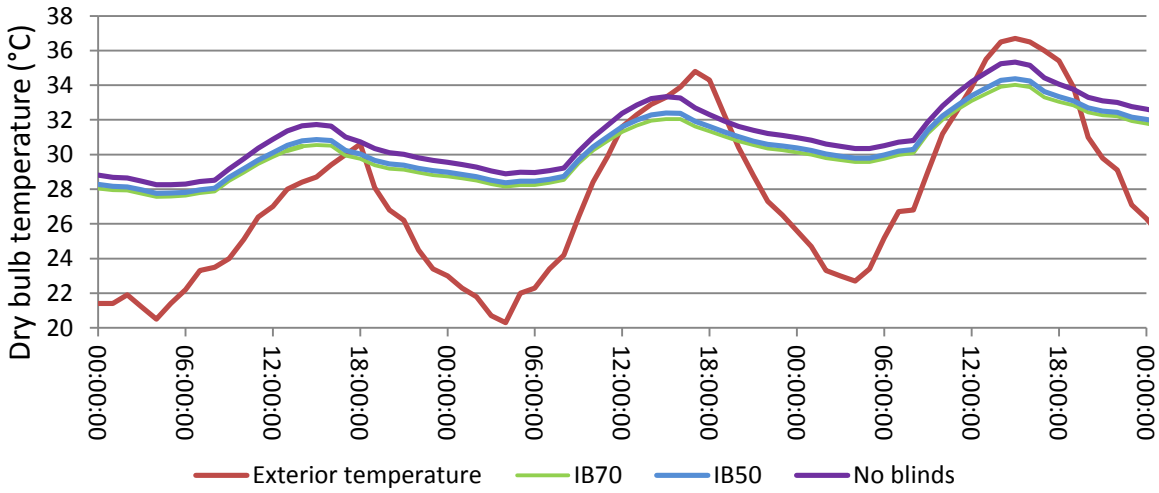

Figure 14: Simulated temperatures from 1st to 3rd August 2013, without blinds, and with internal blinds modelled with the parameters IB50 (50% reflectance) and IB70 (70% reflectance) from Table 4

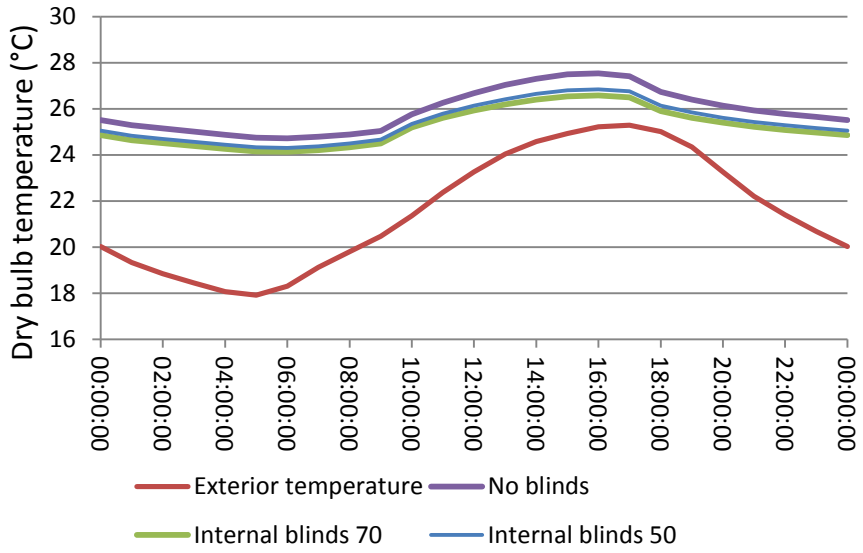

Figure 15: Simulated temperatures, averaged from June to August, without blinds, and with internal blinds modelled with the parameters IB50 and IB70 from Table 4

Figure 16 confirms these results with the mean seasonal overheating, calculated on the same three-month period with formula (15). Internal blinds do lower the mean overheating. The differences between internal blinds of varying coefficients of reflectance are rather limited.

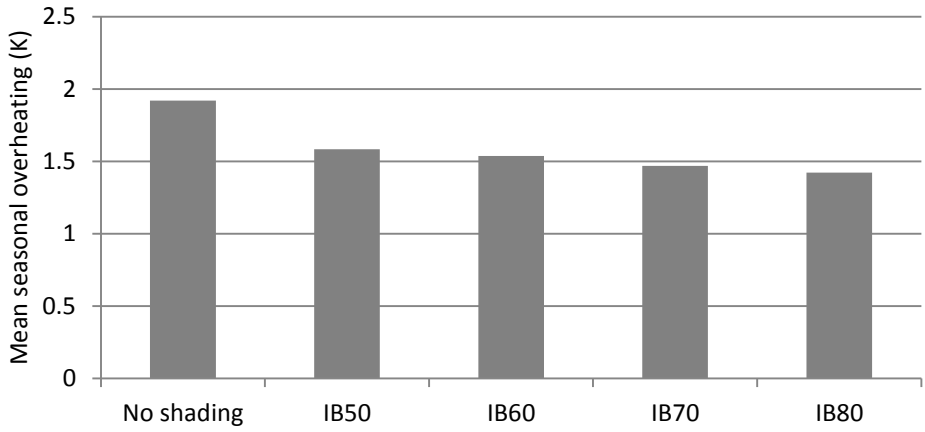

Figure 16: Mean seasonal overheating from June to August, with internal blinds modelled with the different sets of parameters of Table 4

Eventually, similar results apply for the cooling energy demand on the three-month season, as illustrated in Figure 17.

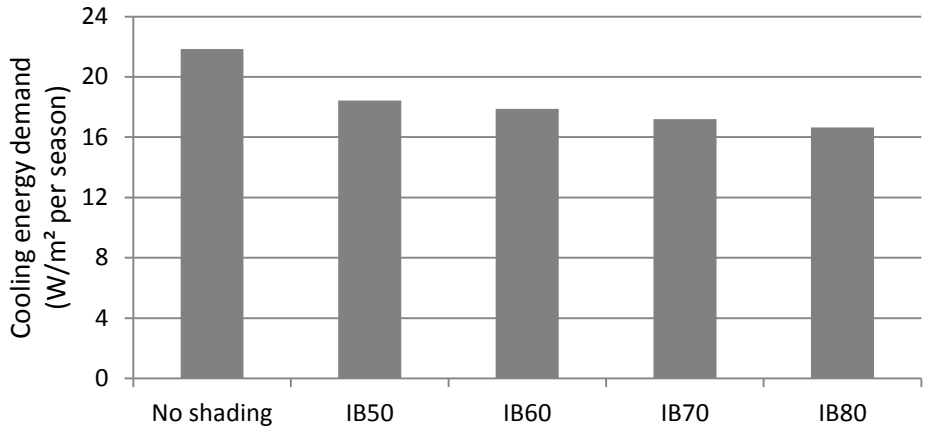

Figure 17: Cooling energy demand from June to August, with internal blinds modelled with the different sets of parameters of Table 4

Results for external blinds

External blinds were simulated in the two different ways that Tas offers: as a "blind" layer in the window construction, or directly from the 3d Modeller. Figure 20 and Figure 21 show a comparison of the results obtained with the two methods. For the first method, case "30-50" of Table 5 was used, with a solar transmittance of 0.30. For the second method, the 3d shade was modelled with dimensions of 180 by 180 cm, with 31 slats of depth 8 cm, at a closed angle of 30°, the slat angle being defined as in Figure 18.

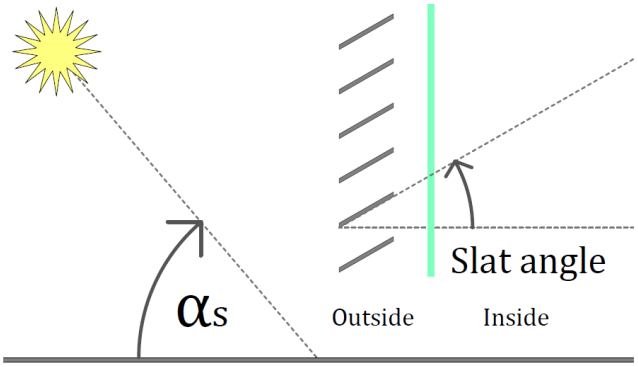

Figure 18: Definition of solar elevation angle α_s and slat angle to the horizontal

Globally, it can be said that the first method leads to a lower estimation of the solar gains, as seen in Figure 20, and consequently to smaller temperatures, as seen in Figure 21.

When entering the shades in the 3d Modeller, one has to choose a certain angle of the slats, which of course plays an important role in the shading performance. Figure 19 confirms the idea that slats tilted in an angle perpendicular to the sun rays work best, around 30 degrees, whereas the biggest cooling energy demand is for slats parallel to them. Horizontal slats are not very far from the optimum, with less than 10% more cooling energy demand.

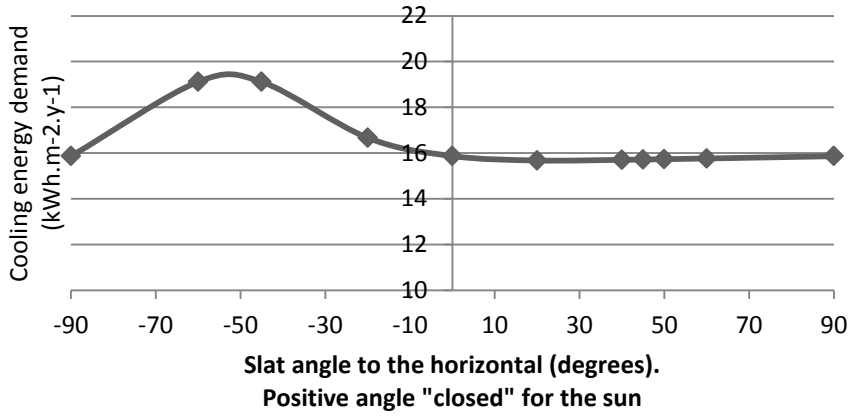

Figure 19: Cooling energy demand for the room equipped with external Venetian blinds, modelled with different slat tilt angles

As expected, solar gains with blinds modelled in the first way are in a direct relation with the solar radiation over the day. On the other hand, when blinds are modelled in 3d, solar gains vary during the day in a way that shows an angle dependency of the solar transmittance.

It can be seen in Figure 20 that blinds modelled in three dimensions are especially poor at shading in the morning (and in the late afternoon). This corresponds to solar energy coming from the sides, and may partly be due to the fact that the blinds are modelled as being 10 cm at the exterior of the wall. But morning and evening also correspond to a higher proportion of diffuse radiation. Diffuse radiation is not shaded in three dimensional shading calculations. With the layer calculations, the same shading applies for diffuse as for direct radiation, which also does not correspond to reality.

The consequence on room temperatures can be seen in Figure 21: since the "layer" shades reduce the solar gains during the whole day, inside temperatures remain accordingly lower. On the other hand, the "3d shading" starts acting later in the day, and the temperature difference is mostly sensible during the warmest hours of the day.

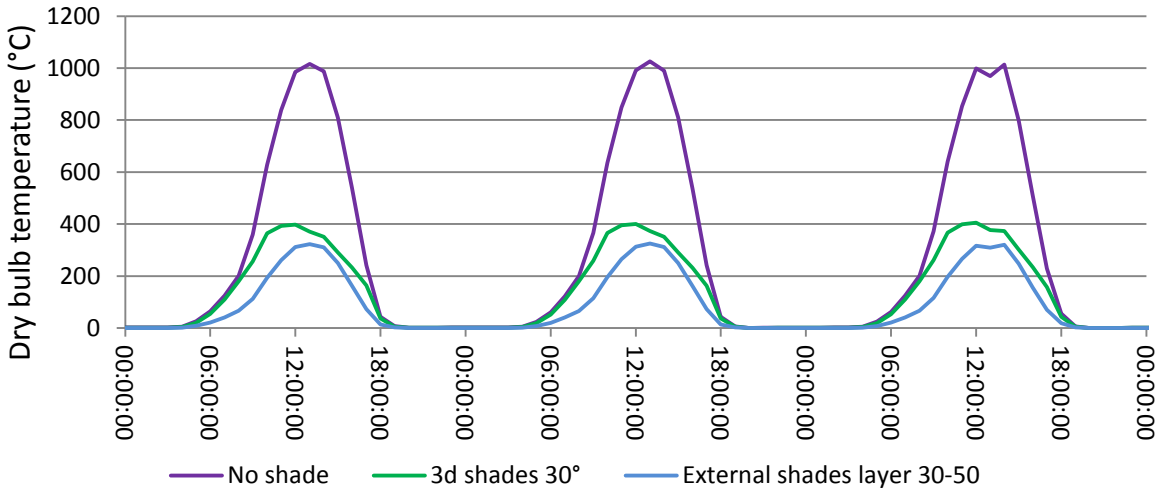

Figure 20: Solar gains (W) from 1st to 3rd August, with external blinds simulated in two different ways, and without shading.

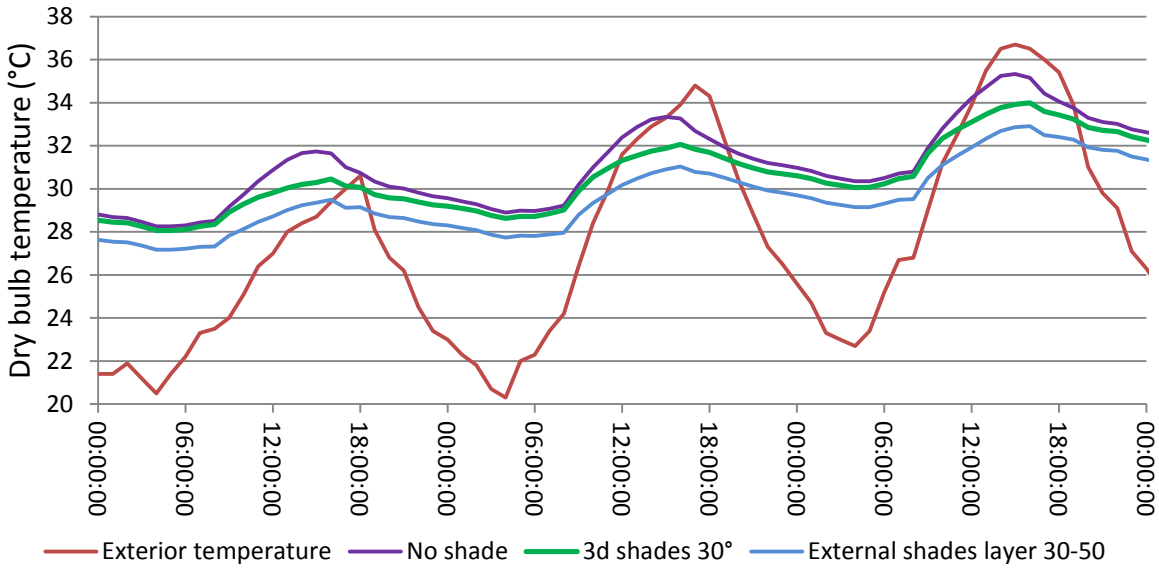

Figure 21: Inside temperature (°C) from 1st to 3rd August, with external blinds simulated in two different ways, and without shading.

The optical-physical properties in the two methods are hardly comparable. In the "blind layer method", they are spatially averaged properties resulting from some previous calculations (see 2.2.3). In this case, high reflectance and high emissivity are always beneficial in preventing heat from entering the room. In the 3d method, the influence of slat properties on the results is much more indirect.

Table 8: Physical properties of different slat materials for external shades

Fin material	Refl 90	Refl 70	Refl 50	Refl 50-70
Solar transmittance	0.00	0.00	0.00	0.00
Int. solar reflectance	0.90	0.70	0.50	0.50
Ext. solar reflectance	0.90	0.70	0.50	0.70
Int. emissivity	0.20	0.90	0.20	0.20
Ext. emissivity	0.20	0.90	0.20	0.90

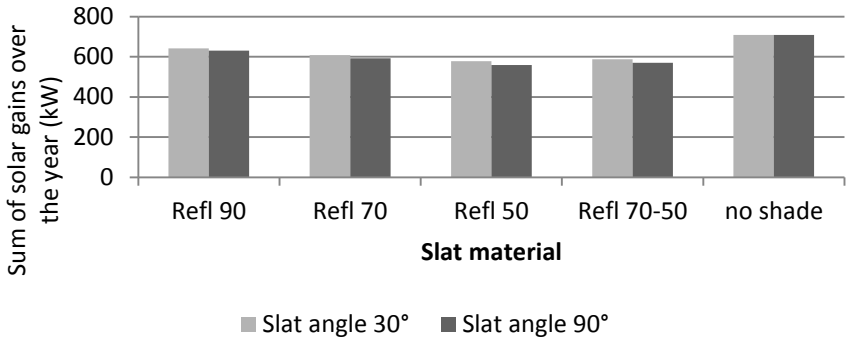

Figure 22: Annual sum of solar gains (kW) in the room with the four different slat materials of Table 8, and without shading

Indeed, radiation can be reflected by a slat onto another one, and end up in the room. The results shown in Figure 22 are not intuitive. Slat materials with a higher reflectance lead to a higher sum of solar gains over the year. For a slat angle of 90°, the blinds are totally closed, so a higher reflectance should minimize solar gains, except for sun beams vertical or lateral enough to reach the blinds "from behind" and be reflected onto the windows.

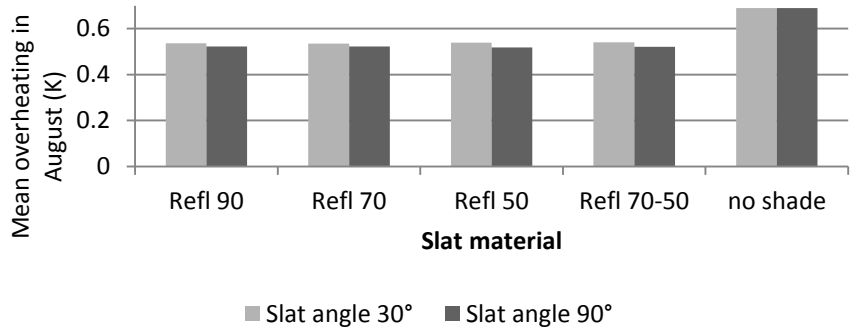

Figure 23: Mean overheating in August, with the four different slat materials of Table 8

Figure 23 shows more logical results: the external blinds with material Refl 70, having higher reflectance and emissivity, perform slightly better for mean overheating than those with Refl 50. However, the difference between the different materials is too small to conclude. These calculations do not take into account the thickness of slats and their thermal properties.

Results for roller shutter curtains

Figure 24 shows that, for totally closed roller shutter curtains, simulations with a feature shade (transmittance of 10%) or with an additional construction layer (properties opaque and translucent from Table 9) provide similar results. In particular, closed roller shutter curtains are quite efficient at minimising the peak of overheating during the warmest hours of the day.

Table 9: Assumed properties of a roller shutter layer

Property	opaque	translucent
Width (mm)	8.9	8.9
Solar transmittance	0.00	0.10
Solar reflectance	0.50	0.50
Emissivity	0.90	0.90
Thermal conductivity (W/m.K)	0.50	0.50

In fact, factors not related to the thermal behaviour speak against roller shutter curtains. They cut the visual contact with the exterior, and prevent daylight from entering the building, which makes their closing for long periods unlikely.

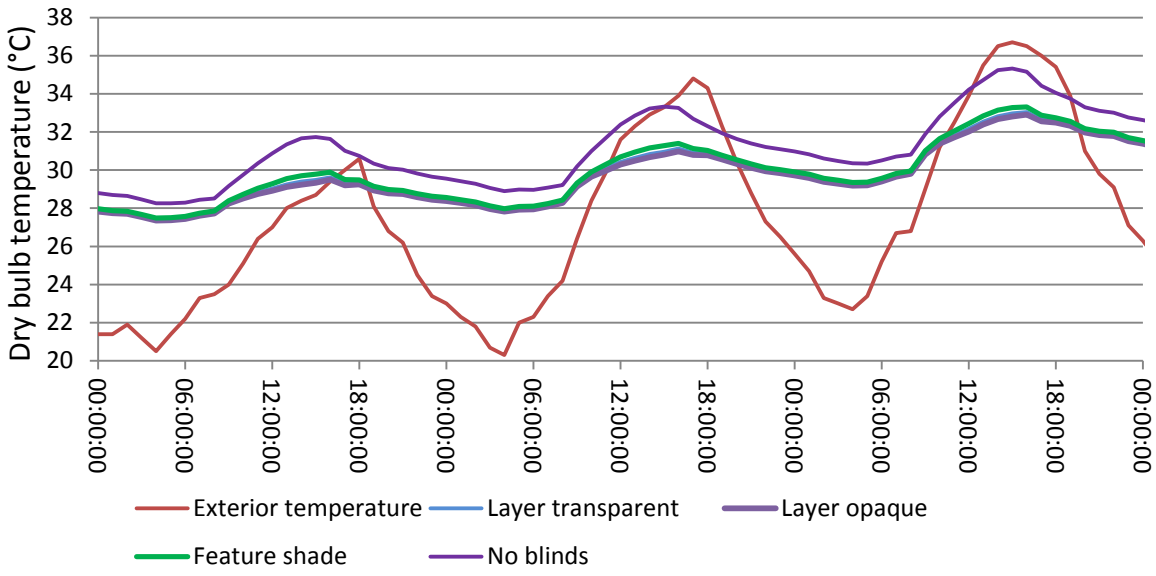

Figure 24: Simulated inside temperature from 1st to 3rd August, without shading, and with totally closed roller shutter curtain, modelled as additional window layer (opaque and transparent from Table 9) and as feature shade

Results for awnings

Awnings simulated as feature shades perform well. Four cases are simulated, corresponding to Table 10. Figure 27 shows that the cooling energy demand can be reduced by almost fifty percent in comparison to the unshaded case.

Table 10: Simulation cases for the awnings. The different arm angles are illustrated in Figure 11

Variable	Case 1	Case 2	Case 3	Case 4
Arm angle (°)	45	30	45	90
Overhang depth (m)	1.08	0.72	1.08	1.46
Overhang offset (m)	-0.48	0.24	-0.48	-1.56
Transmission	0.30	0.10	0.10	0.10

Case 1 and case 3 have the same arm angle of 45°, but different transmission coefficients. Logically, a lower transmission coefficient leads to lower solar gains, as seen in Figure 25, and consequently to lower room temperatures, as seen in Figure 26. Case 2 and case 3 have the same transmission coefficient, but the latter has a higher arm angle, which means it extends lower and blocks more solar radiation, especially during certain hours in the afternoon. The effects of angle and transmission compensate each other for case 1 and 2, so that the resulting room temperatures are almost equal.

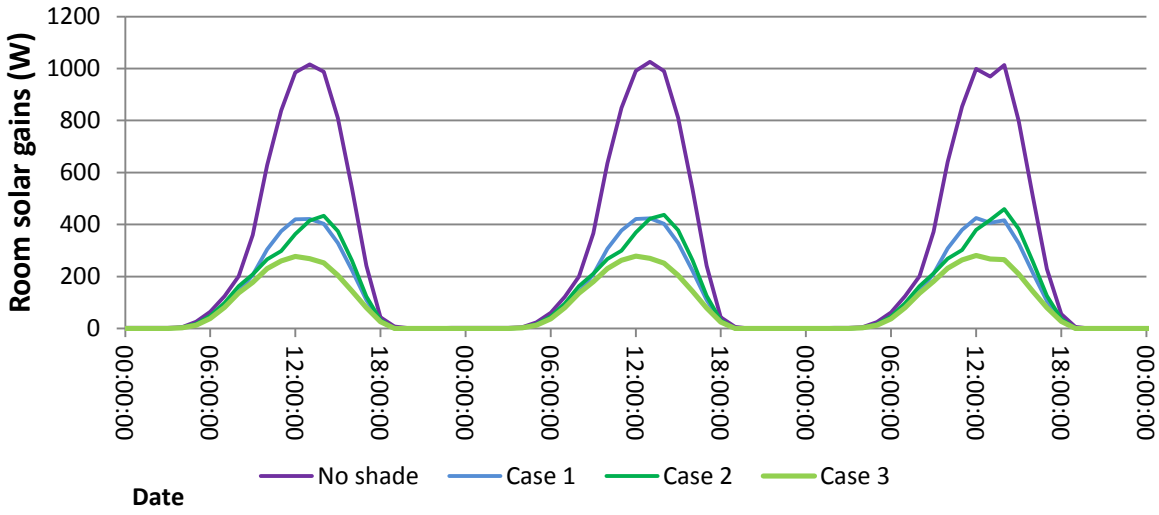

Figure 25: Simulated room solar gains from 1st to 3rd August, respectively without shading, and with awnings cases 1, 2 and 3

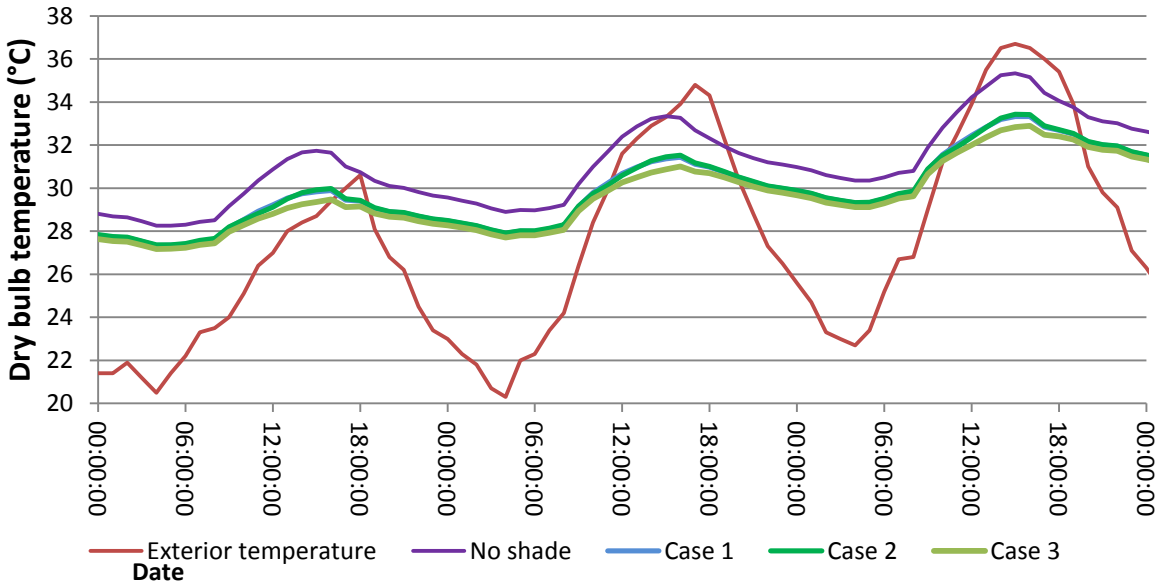

Figure 26: Simulated room temperatures from 1st to 3rd August, respectively without shading, and with awnings cases 1, 2 and 3

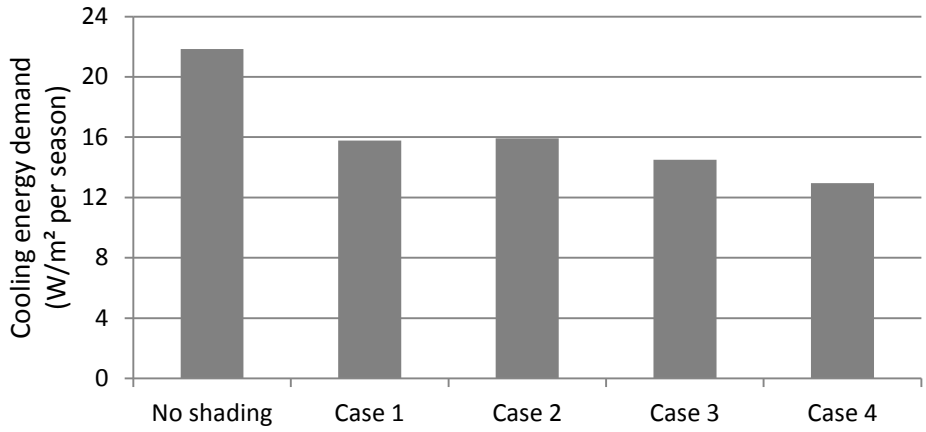

Figure 27: Cooling energy demand from June to August, with awnings modelled with the different cases of Table 10

Results of the comparison between shading systems

Eventually, all shading systems can be compared, by chosing for each one a set of parameters defined in 3.2.4.

Figure 28, with the cooling energy demand, and Figure 29, with the mean overheating for the three-month period, allow for similar conclusions: the cooling energy demand as well as the mean overheating are lower for the room with internal blinds as for the unshaded room. External blinds significantly ameliorate the situation, as do roller shutters and awnings. The results for these three external shading devices are quite similar, so that a slight modification of the input parameters could change their relative position with regards to overheating and cooling energy demand. Similar criteria, such as the number of overheated hours, the maximal temperature, or the peak cooling load, also yield similar results. Eventually, the choice of one of these systems would be more dependent on other criteria. For instance, considering daylighting leads to the exclusion of the roller shutter solution.

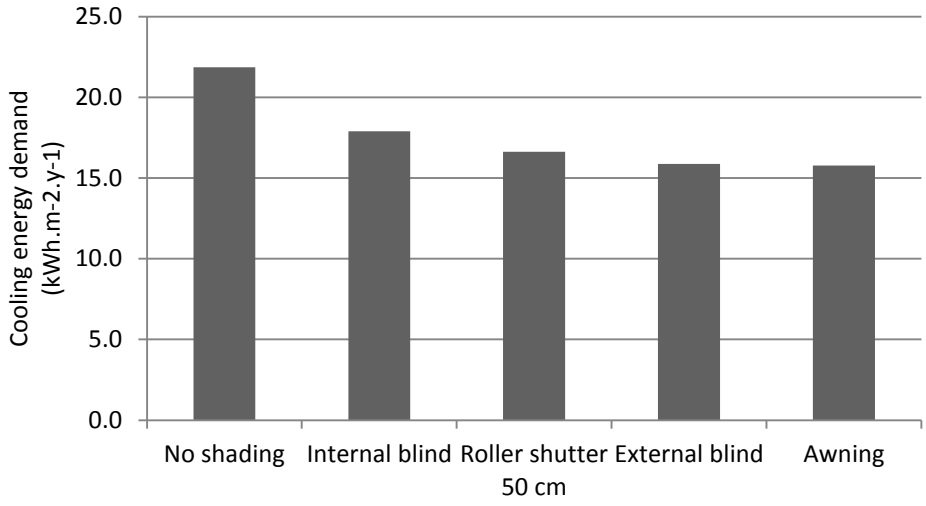

Figure 28: Seasonal (June-August) cooling energy demand for the room with the simulated shading systems

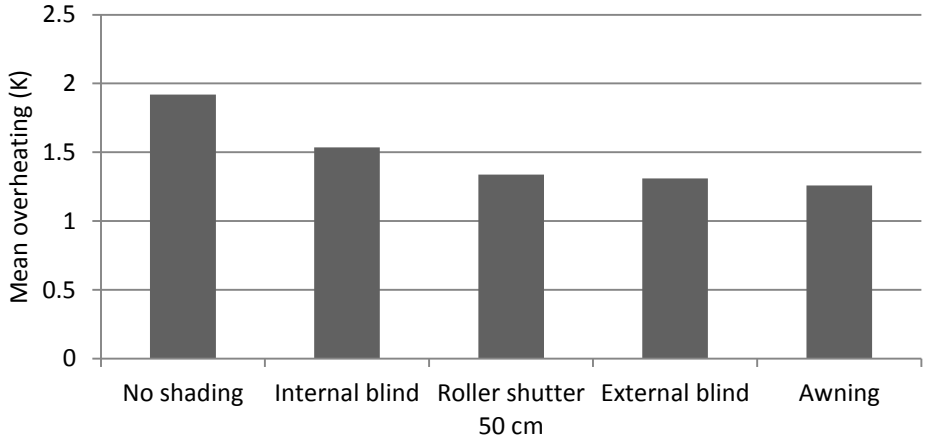

Figure 29: Average mean overheating in June-August for the room with the simulated shading systems

4.2 Results of the monitoring

The temperatures recorded by the different sensors, respectively in the room, in the staircase and in the tower, are respectively presented in Figure 30, Figure 31 and Figure 32. The mean overheating in the room, calculated according to formula (15), amounts to 0.92 K in June, 1.18 K in July, 1.74 K in August, and 0.0 K in September.

The results of SR9 represent a particular case, since the position of this sensor let it receive direct solar radiation, before its displacement to a more appropriate

location. The recorded temperature exhibits peaks of much bigger amplitude than for the other sensors. Apart from SR9, sensors positionned in the same room do have similar temperature curves. However, these curves are offset, temperatures registered by the Hobo sensors being generally of between 1.0 and 1.5 K superior to those registered by the Thermokon sensors, as can be read from Table 11.

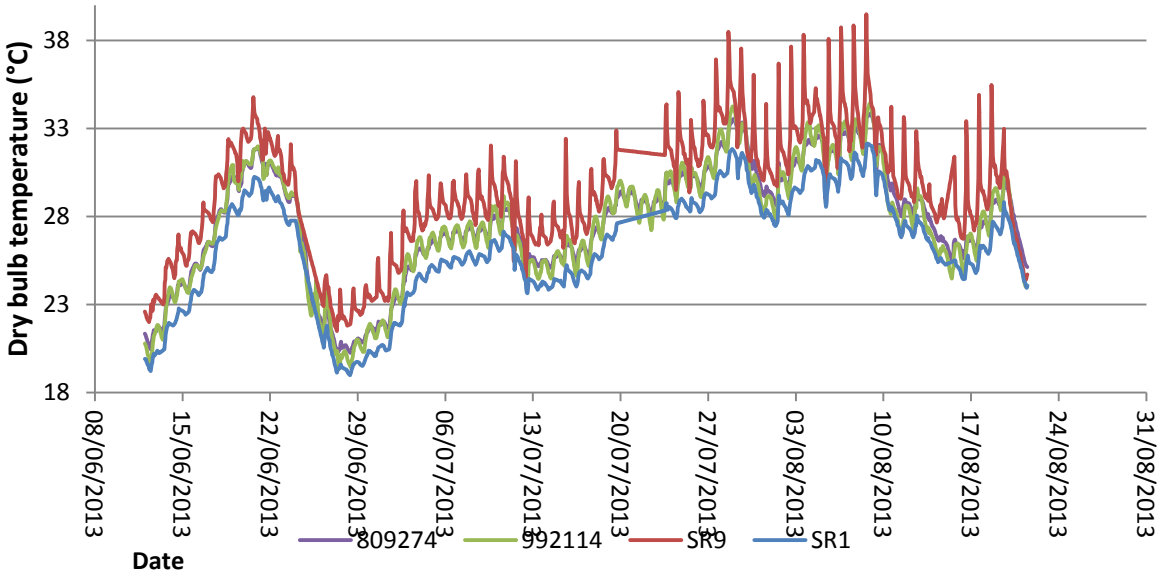

Figure 30: Temperatures recorded by the four sensors in the office room between 8th June and 31th August

Table 11: Estimation of the difference between the temperatures recorded by pairs of sensors placed in the same zone, from 6th June to 19th September

Sensor 1	Sensor 2	Zone	$\overline{\theta^2 - \theta^1}$	$\sigma(\theta^2 - \theta^1)$	RMSE
809164	*SR3*	staircase	1.21 K	0.20 K	1.22 K
809160	*SR2*	tower	1.06 K	0.30 K	1.10 K
809274	*SR1*	room	1.36 K	0.26 K	1.38 K
809274	*992114*	room	-0.12 K	0.43 K	0.45 K
SR1	*SR9*	room	2.63 K	1.11 K	2.85 K

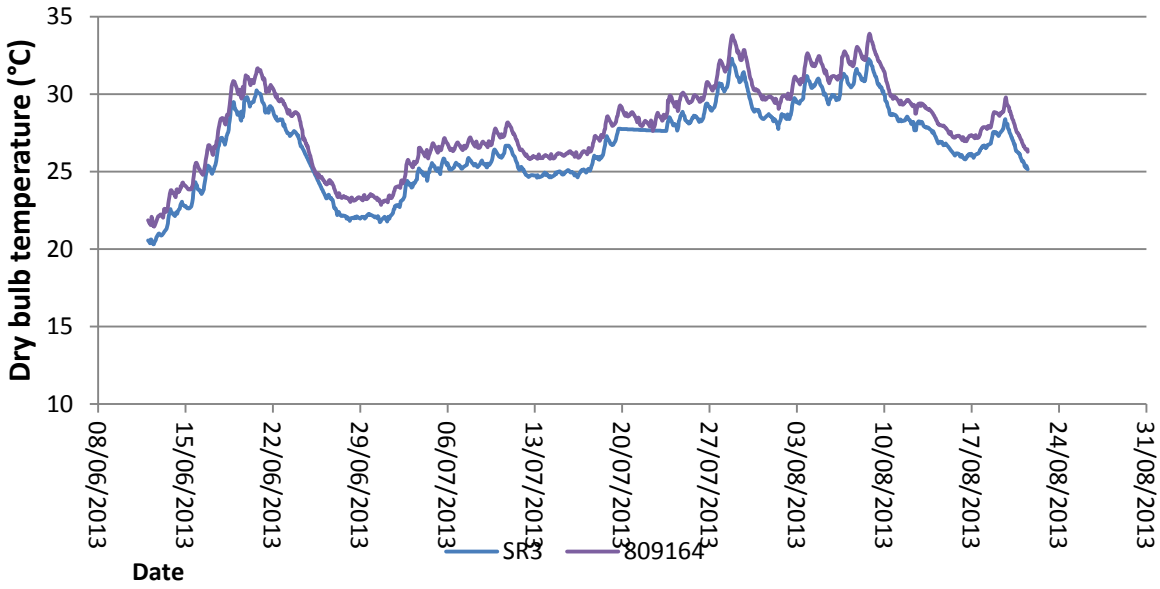

Figure 31: Temperatures recorded by the two sensors in the staircase between 8th June and 31th August

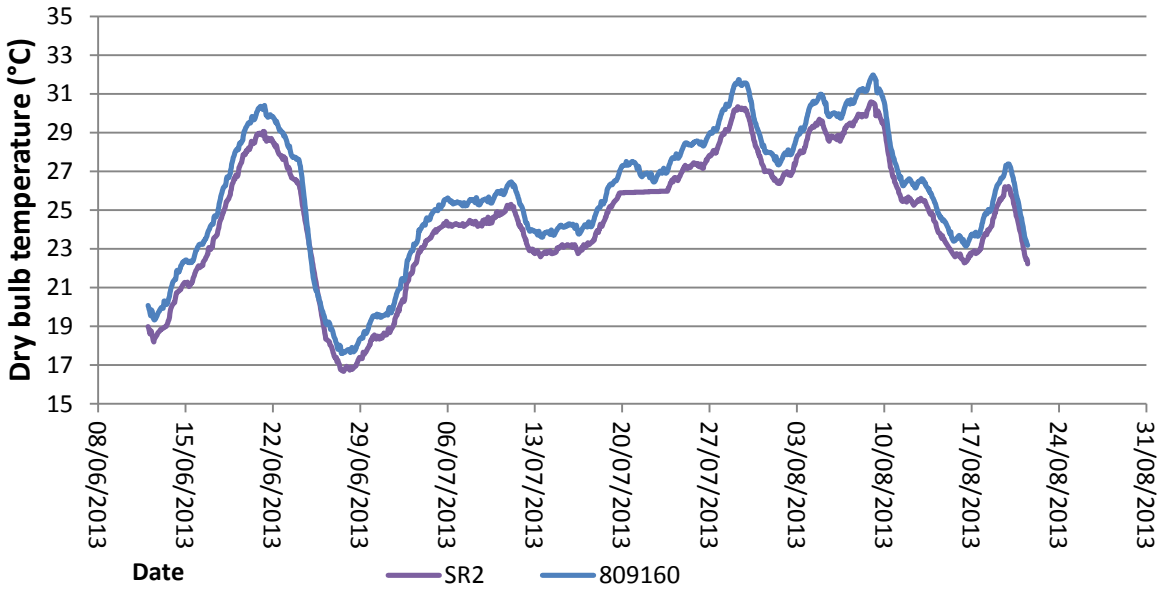

Figure 32: Temperatures recorded by the two sensors in the tower between 8th June and 31th August

The two sensors in the staircase being placed at the same height, a few centimeters apart, temperature stratification can be ignored, and the offset between the two curves is probably due to sensor drift. This is also true of the two sensors placed in the tower zone.

Looking at the results from the sensors placed in the office room, one finds out that the difference between the temperatures recorded by the two hobo sensors 809274 and 992114 is low in average, but features a higher standard deviation than the temperature difference between 809274 and SR1. This could be accounted for by the actual temperature distribution in the room, since 809274 is mounted closer to SR1 than to 992114. Temperatures recorded by SR9 are obviously irregular, because of direct radiation. For all other sensors, which are wall-mounted, it is not clear what influence the wall temperature has on the recorded temperature, making it differ from the air temperature.

Figure 33 shows the monitored values for CO2 concentration, window contact and occupancy in the room. It is possible to make out a certain correlation, the CO2 concentration increasing in the room when it is occupied, all the more if the windows are not opened. Occupancy and window contact values are recorded at irregular times, when a variation is detected. This data then has to be converted into hourly values for use in dynamic simulation in step 2 of the calibration.

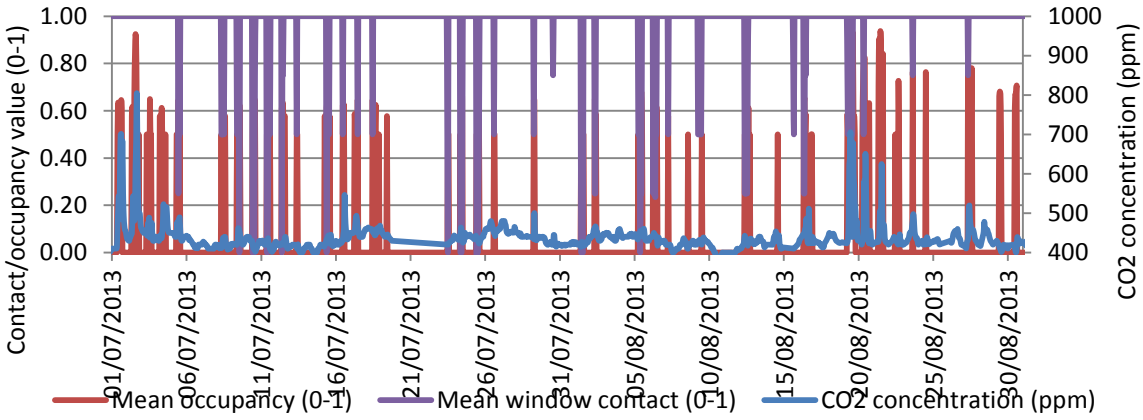

Figure 33: Monitored CO2 concentration (ppm), window contact (average of four sensor values) and occupancy (average of two sensor values)

4.3 Calibration of the unshaded room

The calibration process begins with the unshaded room, as monitored in the first period. We start simulations with a set of simple parameters, corresponding to

null internal gains, and an infiltration rate of 0.6 ach in each of the three zones (first row in Table 12).

Table 12: Simulation parameters at different steps of the calibration process. Step 0: before calibration. Step 1: calibration with fixed parameters. Step 2: calibration with parameters derived from occupancy and window contact monitoring

Parameter	Step 0	Step 1	Step 2
Number of zones	3	4	4
Self-shading	no	yes	yes
Infiltration room (ach)	0.6	0.1	0.1
Infiltration tower (ach)	0.6	0.25	0.25
Infiltration staircase (ach)	0.6	0.2	0.2
Room sensible gain (W/m²)	0.0	0.0	4.occ
Room latent gain (W/m²)	0.0	0.0	2.occ
Room equipment gain (W/m²)	0.0	1.2	1.2 + 6.occ
Staircase lighting gain (W/m²)	0.0	1.8	1.8
4th Zone internal gain (W/m²)	-	12.0	12.0
Ground reflectance	0.40	0.15	0.15
Windows opening	None	None	Yes

Comparing the monitored temperatures and the temperatures simulated with this first set of parameters, in Figure 34, one sees that the progression on larger periods of time is quite similar, but that the behaviour on a daily basis is different. In particular, the simulated temperatures display much larger daily oscillations than what is measured.

In this first part of the calibration, it was decided to base comparisons on the Hobo sensor 809274 for measured temperatures, and on an average of the dry bulb temperature and of the inside surface temperature of the external wall for the simulated temperatures. This is based on the assumption that the sensor measurement is significantly influenced by the temperature of the wall on which it is mounted.

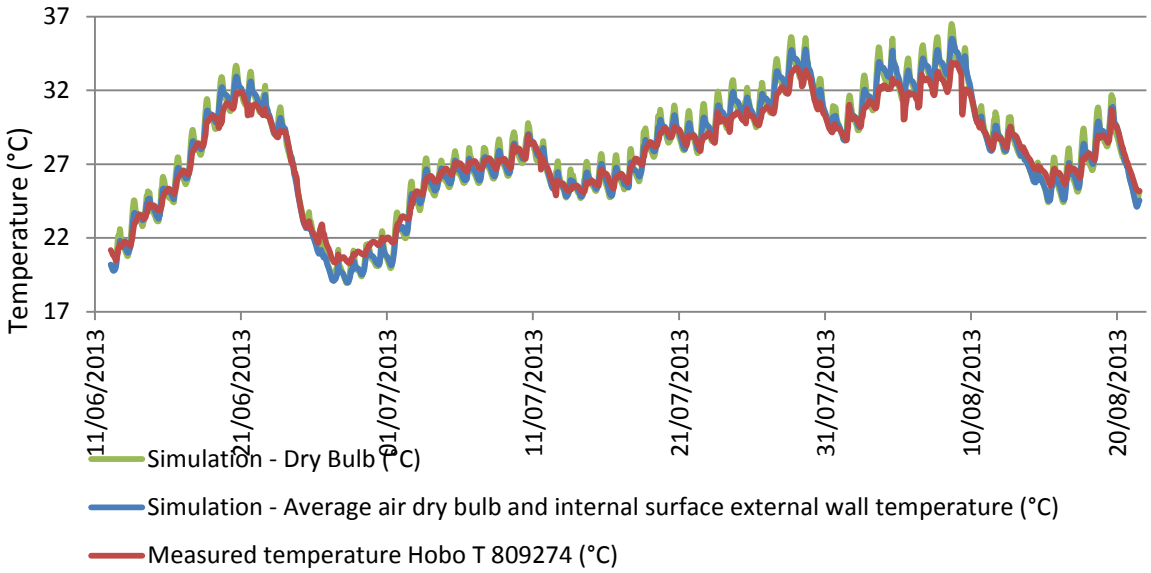

Figure 34: Monitored temperatures (in red) against temperatures simulated before calibration (with parameters of step 0 in table 11) in green and blue, from 12th June to 20th August

In order to obtain a better match between monitored and simulated temperatures, the first calibration step consisted in modifications of the infiltration rates and the internal gains in the three zones, as well as in the addition of a fourth zone under the staircase zone. Some feature shading was also added to the windows to account for self shading of the building (15 cm laterally, and 30 cm on top). The construction layers were not changed. The creation of a fourth zone was motivated by the inadequacy of the simulation for the staircase zone in step 0, and the obvious coupling of the different zones of the staircase.

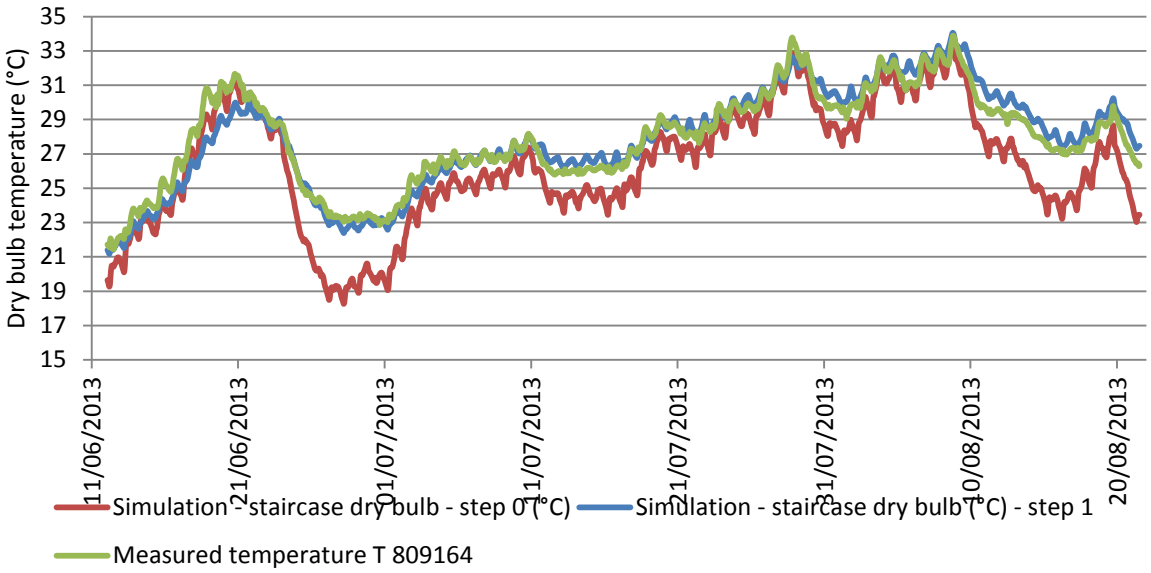

Figure 35: Measured temperatures against simulated temperatures in the staircase, for steps 0 and 1 of the calibration

In a second step, the monitoring data concerning the room occupancy and the opening of windows has been used to specify hourly values of internal gains and window openings in order to reach a better consistancy.

At the end of this second step of calibration, the heat gain coefficients for the occupancy are $g^{sensible} = 4.0\ W.m^{-2}$ and $g^{latent} = 2.0\ W.m^{-2}$. For the mean opening k in formula (8), a value of 0.20 was found to yield the best results.

Concerning the indicators evaluating the error in simulated values as compared to measured values, Table 13 shows that the goodness-of-fit increases at each calibration step, except for the tower zone indicator. These values can be compared to the values of Table 11 estimating the difference between temperatures recorded by pairs of sensors placed in the same room. The value of the root mean square error obtained for the room after the second step of calibration is close to the accuracy of the sensors (±0.35 K).

Table 13: Values of the indicators for the different steps of calibration, calculated on the period 12th June-20th August

Indicator	Zone	Step 0	Step 1	Step 2
$\overline{\boldsymbol{\theta^s - \theta^m}}$	room	0.09 K	-0.26 K	-0.15 K
$\boldsymbol{\sigma(\theta^s - \theta^m)}$	room	0.71 K	0.47 K	0.41 K
$\boldsymbol{max(\lvert\theta^s - \theta^m\rvert)}$	room	3.10 K	2.93 K	1.84 K
$\boldsymbol{RMSE}$	room	0.71 K	0.54 K	0.43 K
$\boldsymbol{RMSE}$	staircase	2.56 K	0.73 K	0.70 K
$\boldsymbol{RMSE}$	tower	0.88 K	0.69 K	0.70 K

Figure 36 shows that simulated temperatures and monitored temperatures in the office room fit variably well according to the period. For instance, there is a better than average fit on the period from 27th July to 1st August, as show the values of the error indicators in Table 14, when compared to the values of the whole monitoring period found in Table 13. Figure 37 also shows a particularly good fit on this period.

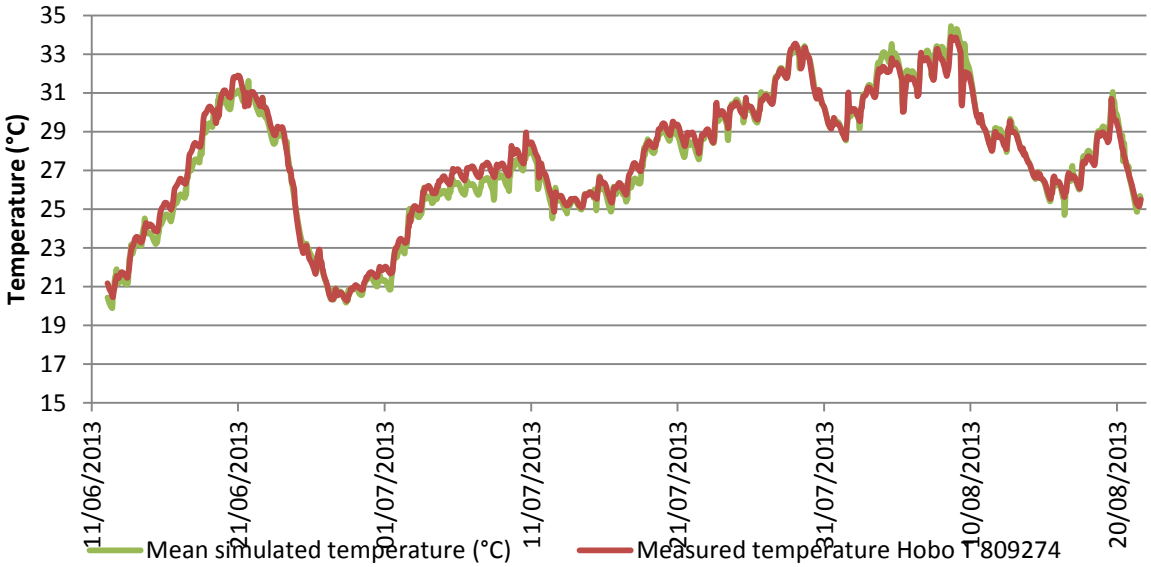

Figure 36: Simulated temperature (mean dry bulb and wall temperature, calibration step 2) and measured temperature in the office room, from 12th June to 20th August

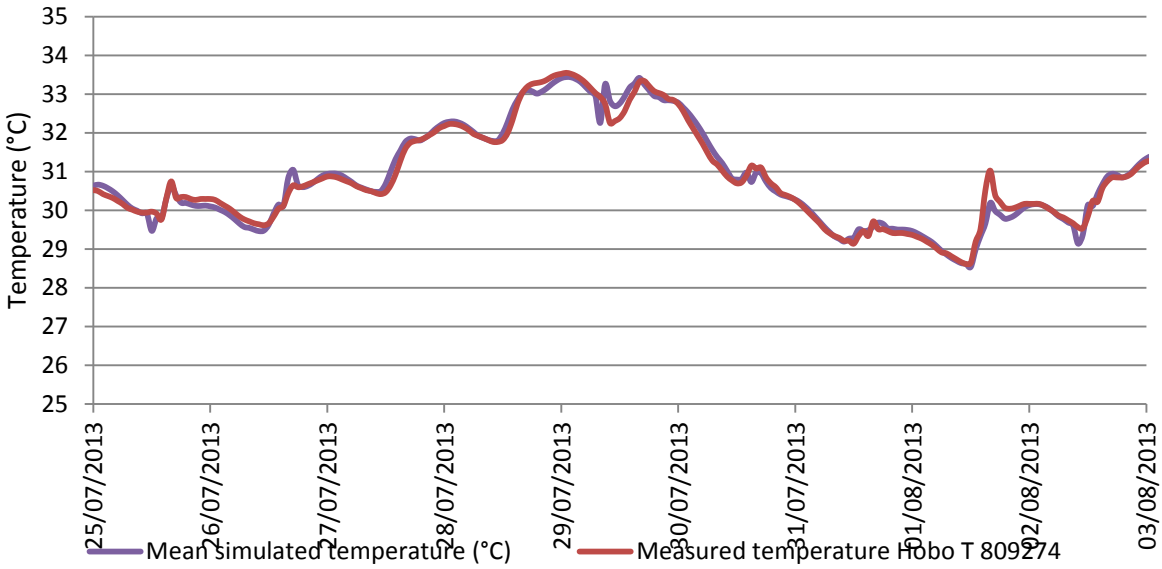

Figure 37: Measured temperature in the office room against simulated temperature after calibration (step 2), from 25th July to 3rd August

Table 14: Values of the indicators for the different steps of calibration, calculated on the period 27th July-1st August

Indicator	Zone	Step 0	Step 1	Step 2
$\overline{\boldsymbol{\theta^s - \theta^m}}$	room	0.62 K	0.04 K	0.05 K
$\boldsymbol{\sigma(\theta^s - \theta^m)}$	room	0.47 K	0.14 K	0.17 K
$\boldsymbol{max(\lvert\theta^s - \theta^m\rvert)}$	room	1.66 K	0.45 K	0.67 K
$\boldsymbol{RMSE}$	room	0.78 K	0.14 K	0.17 K

The staircase zone is the one with the largest error. This is also the zone where internal conditions are the most difficult to evaluate. Figure 38 shows that the fit for the tower zone is globally good, but simulated temperatures oscillate more inside of a day than is monitored.

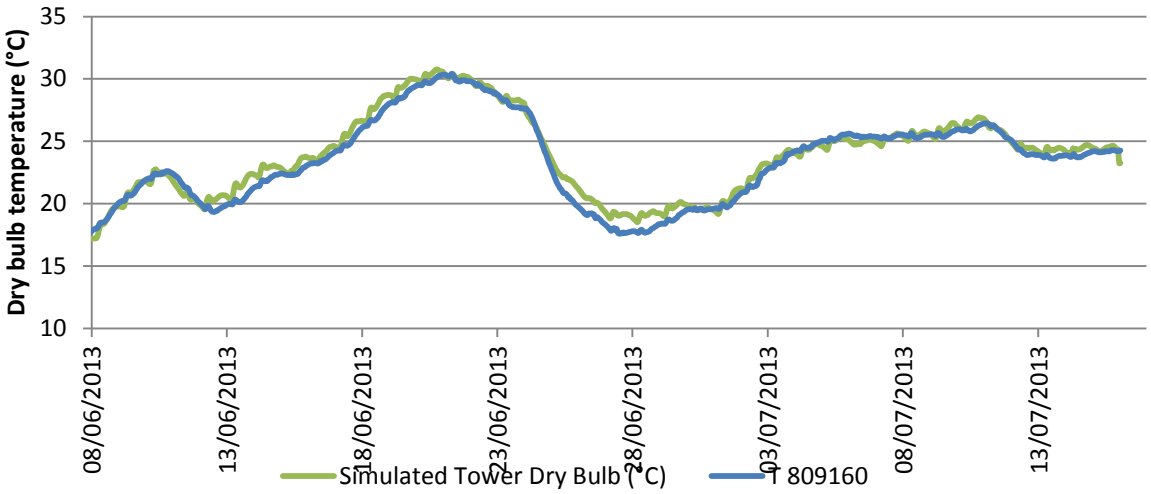

Figure 38: Simulated temperature (dry bulb) and measured temperature in the tower zone, from 8th June to 15th July

Limitations of the calibration

Beyond the inaccuracies in the monitoring of occupancy and window opening, there are unknowns in the operation of the room which limit the calibration. The opening of the doors to the tower and to the staircase was not monitored. During the hot period, the door to the tower was some times opened for longer periods. Also, the small server cabinet adjacent to the room might have been an important source of internal gains, which could not be assessed. It has only been taken into account by the constant equipment gain in the room determined during the calibration.

4.4 *Calibration of the room with Venetian blinds*

Based on the calibration for the unshaded room, it was then possible to calibrate the simulation of the room equipped with shades, by tweaking shading-related parameters while considering other parameters fixed.

4.4.1 Calibration of the room with interior Venetian blinds

The interior Venetian blinds were drawn down from 20th August to 11th September. Because of overcast weather, the period was not entirely relevant for our study.

The five-day interval from 6th to 10th September was chosen for the calibration of the simulation with interior Venetian blinds. For this period, a comparison of the results from the calibrated simulation without shading (green in Figure 39) with the monitored temperatures (red in Figure 39) shows that the interior blinds actually tend to yield lower indoor temperatures, with a mean temperature difference of 0.8 K. This difference is comparable to the mean error. Also, it is not noticeable on previous days with less radiation, for which the effect of internal blinds does not appear.

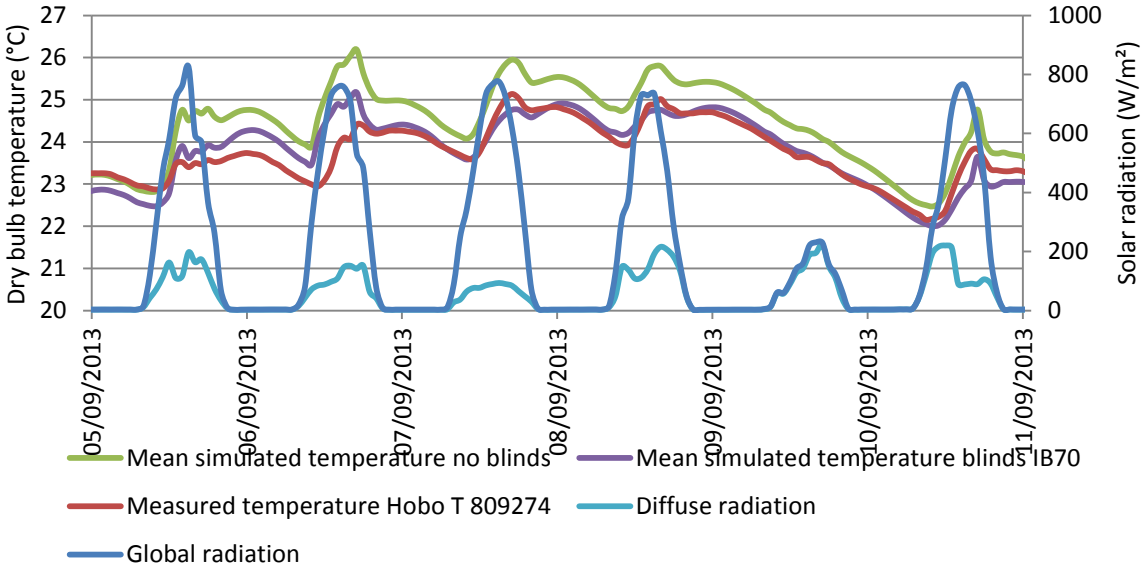

Figure 39: Monitored temperature (red) against temperatures simulated with element substitution accounting for internal blinds IB70 (violet) and without substitution (green), from 6th to 10th September

Still, the temperature difference obtained when trying to account for this difference by the simulation of internal blinds is even smaller. The calibrated simulation was run again with the different internal blind parameters introduced in 3.2.4, with method 1.

With a sensor accuracy of ±0.35 K, it is difficult to conclude on the effect of internal blinds on the temperature in the room, as well as to calibrate the simulation with regard to these shading systems. The values of indicators grouped in Table 15 seem to agree with the modelling with the parameters IB70.

Table 15: Temperature error indicators for the period 6th to 10th September

Indicator	No shading	IB60	IB70	IB80
$\overline{\theta^s - \theta^m}$	0.81 K	0.19 K	0.07 K	-0.03 K
$\sigma(\theta^s - \theta^m)$	0.33 K	0.33 K	0.33 K	0.35 K
$max(\lvert\theta^s - \theta^m\rvert)$	2.04 K	1.42 K	1.33 K	1.24 K
$RMSE$	0.87 K	0.38 K	0.35 K	0.35 K

4.4.2 Calibration of the room with exterior Venetian blinds

The exterior Venetian blinds were drawn down from 08:00 to 17:00 on 19th and 20th September, and from 23rd to 28th September.

From Figure 40, it appears that the measured temperature generally does not rise when the external blinds are closed. A similar behaviour of the simulated temperature can be achieved by the simulation of the external blinds with the layer method. Layer properties "30-50" and "15-50" are assumed, with a reflectance of 0.50, and a transmittance of respectively 0.30 and 0.15. Comparing this with the simulation without blinds, one can evaluate the effect they have on the room temperature. The temperature is indeed lower when blinds are simulated, and blinds with a lower transmittance do lead to lower simulated temperatures. On the whole, neither Figure 40, nor Table 16, which regroups the temperature error indicators, makes it clear which assumption leads to a better fit.

Unpredicted heat gains due to the activating of a radiator interfere with the comparison on 24th and 25th September. Globally, the quality of the calibration is inferior to that achieved in July and August for the unshaded room. This could be partially justified by different user patterns at the university at the end of the holidays, and by the beginning of the heating period in the lower floors.

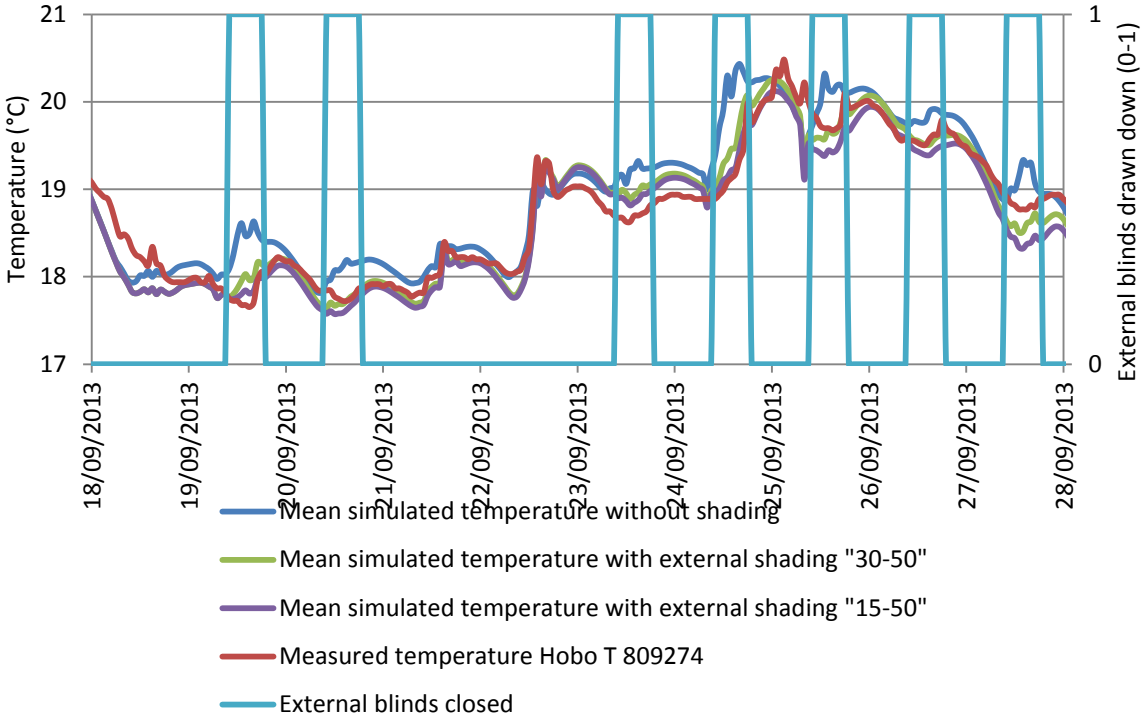

Figure 40: Measured temperatures from 18th to 28th September, against simulated temperatures, with and without simulation of external shading

Table 16: Temperature error indicators for the period 19th to 28th September

Indicator	No shading	EB 30-50	EB 15-50
$\overline{\boldsymbol{\theta^s - \theta^m}}$	0.28	0.07	-0.01
$\boldsymbol{\sigma(\theta^s - \theta^m)}$	0.41	0.33	0.34
$\boldsymbol{max(\lvert\theta^s - \theta^m\rvert)}$	1.32	1.12	1.09
$\boldsymbol{RMSE}$	0.50	0.34	0.34

4.5 Calibrated simulation of the effects of Venetian blinds

Despite the difficulties encountered in the calibration of the dynamic simulation of the room with shading systems, one can feed the resulting parameters back to the simulation of the whole period, in order to get a broader evaluation of the effects of these shading systems, for longer periods of use. Table 17 sums up different parameters of the calibrated model. Simulations are carried out for two different window types: low-e windows such as are present in the actual room and "normal" clear double glazing windows. Only parameters related to the windows differ. Apart from the air change rate in the office room and the room internal gains, the remaining parameters all correspond to the results of the calibration, described in 4.3 for the unshaded room and in 4.4 for the blinds.

Table 17: Calibrated simulation parameters for low-e windows and normal windows

Parameter	Low-e windows	Normal windows
Internal blinds	IB70	IB70
External blinds	EB15-50	EB15-50
Glazing U-value (W/m².K)	1.1	2.6
Unshaded glazing g-value	0.76	0.63
Infiltration room (ach)	1.0	1.0
Infiltration tower (ach)	0.25	0.25
Infiltration staircase (ach)	0.2	0.2
Room internal gain (W/m²)	4.75	4.75
Room gain schedule	9:00-17:00	9:00-17:00
Staircase internal gain (W/m²)	1.8	1.8
Ground reflectance	0.15	0.15

Figure 41 and Figure 42 show the simulated room temperatures after calibration, from 1st to 3rd August 2013, respectively with low-e and normal windows. Figure 43 and Figure 44 show the simulated temperatures for a synthetic day averaged on the 3-month period, respectively with low-e and normal windows. The same conclusions apply as before the calibration. Internal blinds lower the room temperature, and external blinds also do, but more significantly. The effects of blinds are more important for normal windows than for low-e windows, which already block more of the solar radiation. The higher U-value of normal windows also plays a certain role, in facilitating night-time natural cooling.

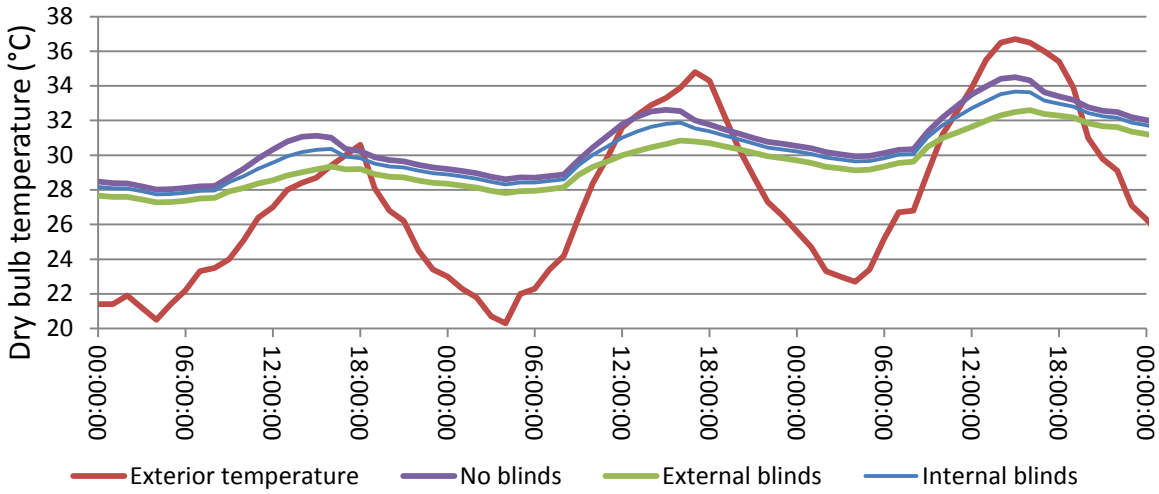

Figure 41: Simulated temperature in the office room from 1st to 3rd August 2013, after calibration and with low-e windows such as in the actual room

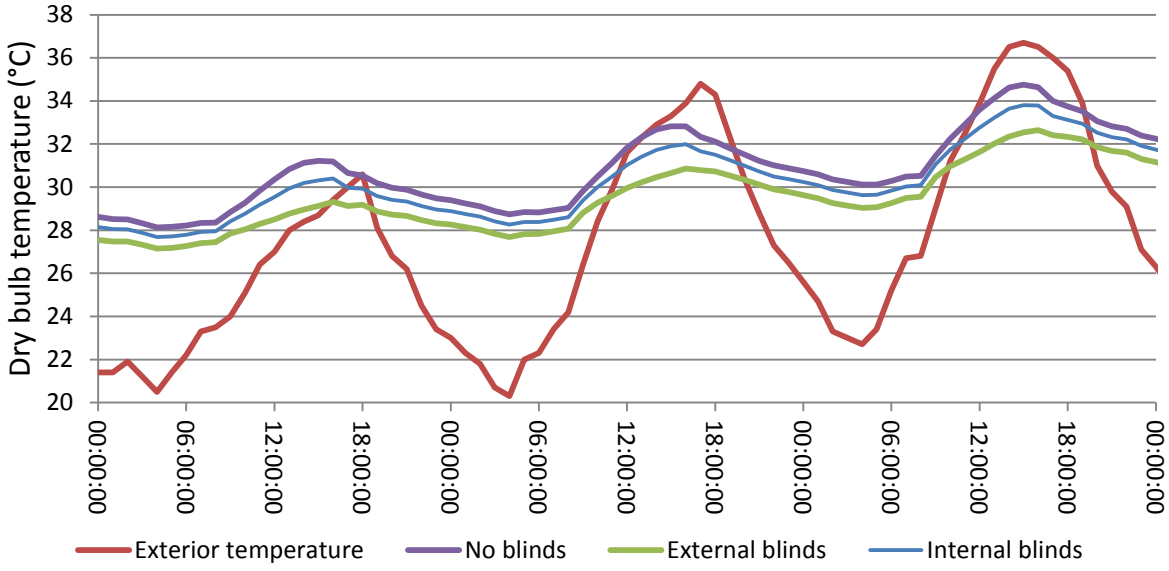

Figure 42: Simulated temperature in the office room from 1st to 3rd August 2013, after calibration and with clear double glazing windows

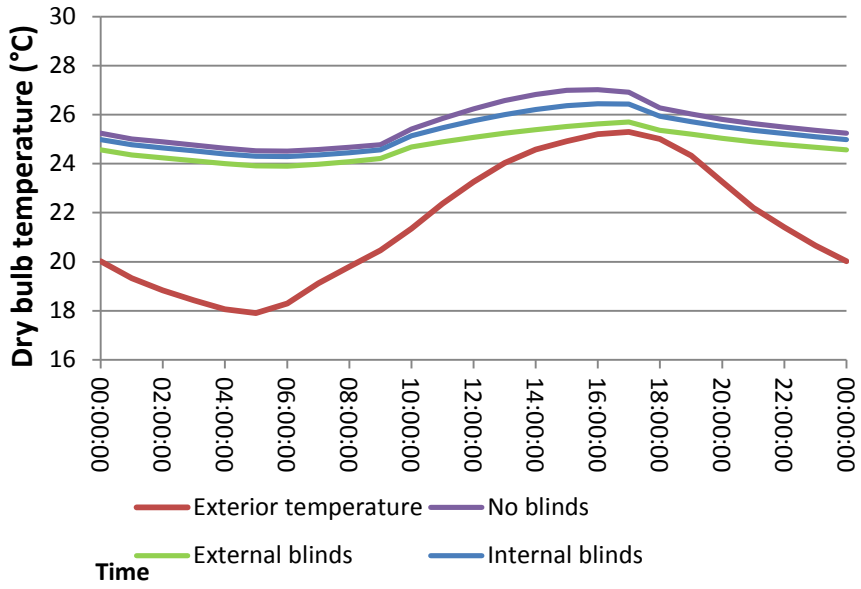

Figure 43: Simulated temperature in the office room averaged from June to August, after calibration and with low-e windows such as in the actual room

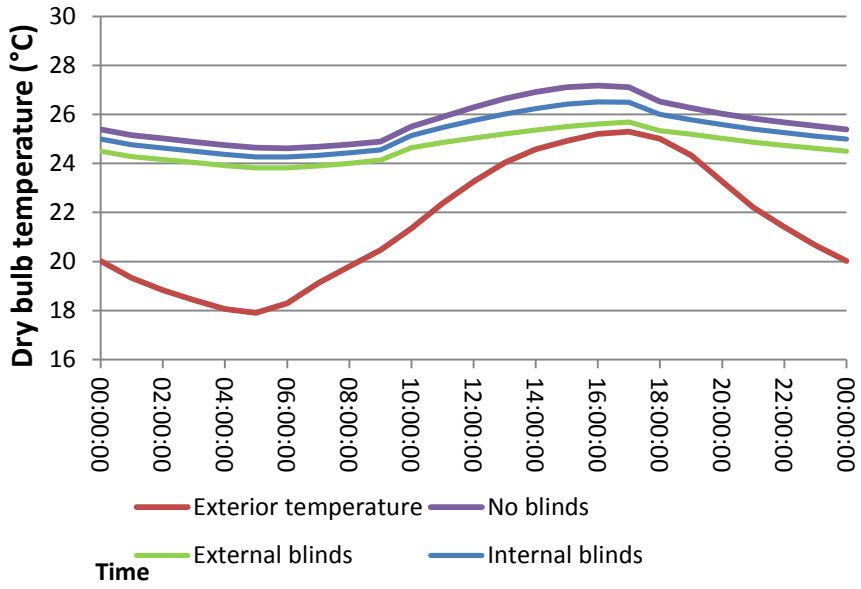

Figure 44: Simulated temperature in the office room averaged from June to August, after calibration and with clear double glazing windows

Figure 45 and Figure 46 compare cooling energy demand and mean overheating for the three shading situations (no shading, internal blinds, and external blinds) and two types of windows: low-e windows and normal windows. In every case, shading devices reduce the cooling energy demand as well as the mean overheating over the season. Also, the decrease in cooling energy demand and in

mean overheating is significantly more important with external Venetian blinds than with internal Venetian blinds. The comparison between low-e windows and "normal windows" confirms the trend exposed with the previous temperature curves: the relative effect of shading devices is more important when they are applied on normal windows than when they are applied on low-e windows as those present in the actual room.

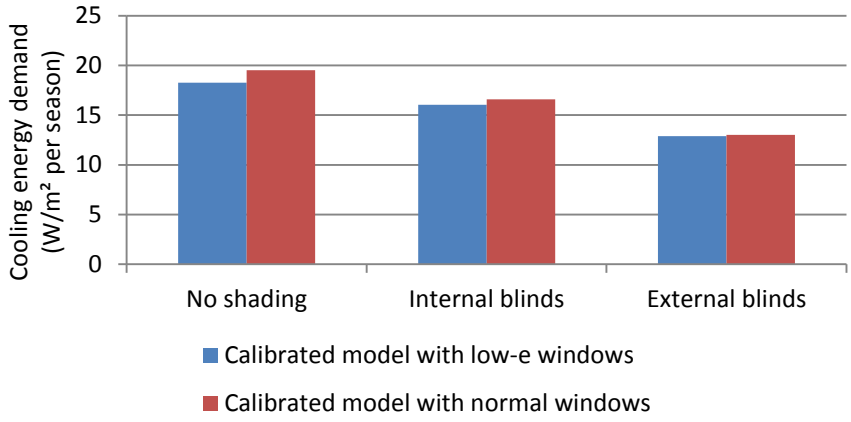

Figure 45: Mean seasonal cooling energy demand (from June to August) for the calibrated model, with low-e windows and with normal windows.

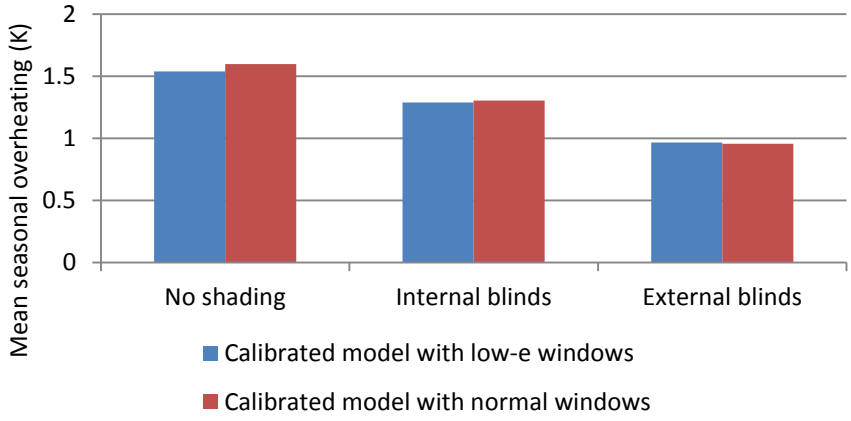

Figure 46: Mean seasonal overheating (from June to August) for the calibrated model, with low-e windows and with normal windows.

Chapter 5

Conclusion

The results suggest that monitoring and dynamic building simulation are indeed complementary in the evaluation of the thermal effects of shading systems. Calibration can improve the predictive performance of dynamic building simulation. However, this improvement is more significant for the unshaded room than for the room equipped with shading devices.

Calibration of the unshaded building is a necessary step. The availability of more data from the manufacturers of shading devices would probably attenuate the degree of necessity of the second step of calibration. In this regard, the main issue is the dependance of the total energy transmittance of a shaded window on a number of parameters, including the glazing properties, the incoming radiation, and, for louvered systems, the slat angle. Still, this should not prevent meaningful values to be determined for well-defined, although limited situations. Alternatively, the disclosure of the physical and optical properties of the shading materials makes calculations possible for any case. Still, the tool for these calculations was not included in the software used for this work, and it was not possible to fully use results from an external tool. Among other limitations, the tool is restricted to two configurations for substitute elements, and to fixed shading systems for 3d shading calculations.

After this last step of calibration is completed, the calibrated model could prove useful as well for the choice of similar devices in other situations as for the operation of the actual device in an optimal way. There again, this would require a tool with less restrictions with regard to the simulation of shading systems.

Chapter 6

References

6.1 Literature

ASHRAE, 2009. *ASHRAE Handbook - Fundamentals.* s.l.:s.n.

Bartl, J. & Baranek, M., 2004. Emissivity of aluminium and its importance for radiometric measurement. *Measurement of Physical Quantities,* Volume 43, pp. 31-36.

Bayraktar, N. T. & Ok, V., 2009. A method for evaluating external shading device influences on zone gains by EnergyPlus simulation programme. *Proceedings Eleventh International IBPSA Conference,* pp. 984-991.

Beausoleil-Morrison, I., 2000. *The adaptive coupling of heat and air flow modelling within dynamic whole-building simulation,* s.l.: Ph.D. dissertation, University of Strathclyde.

Bou Saada, T. & Haberl, J., 1995. An improved procedure for developing calibrated hourly simulation models.. *Proceedings of the International Building Performance Simulation Association, August 14-16, 1995,* pp. 475-484.

Bull, K., 2008. Thermistors and Thermocouples: Matching the Tool to the Task in Thermal Validation. *The Journal of Validation Technology,* Issue 14 (Winter).

CEN, 1998. EN 410: *Glass in building - Determination of luminous and solar characteristics of glazing.* Brussels: European Committee for Standardization

CEN, 2005. prEN 14501: *Blinds and shutters - Thermal and visual comfort - Performance and characteristics and classification.* Brussels: European Committee for Standardization

CEN, 2006. EN 13363-2: *Solar protection devices combined with glazing - Calculation of total solar energy transmittance and light transmittance - Part 2: Detailed calculation method.* Brussels: European Committee for Standardization

CEN, 2009. EN 13363-1: *Solar protection devices combined with glazing - Solar protection devices combined with glazing – Calculation of solar and*

light transmittance - Part 1: Simplified method. Brussels: European Committee for Standardization

Clarke, J., Strachan, P. & Pernot, C., 1993. An approach to the calibration of building energy simulation models.. *ASHRAE Transactions,* Volume 99, pp. 917-917.

Clark, J., Peeters, L. & Novoselac, A., 2013. Experimental study of convective heat transfer from windows with Venetian blinds. *Building and Environment,* Volume 59, pp. 690-700.

Collins, M. & Harrisson, S., 2004. Estimating the Solar Heat and Thermal Gain from a Window with an Interior Venetian Blind. *ASHRAE Transactions,* 110(1), pp. 486-500.

Dubois, M. C., 1997. *Solar Shading and Building Energy Use. A Literature Review,* Lund: Lund University.

Duška, M. et al., 2007. Trend in heat gains from office equipment. *Proceedings of Indoor Climate of Buildings, Strbske Pleso,* 6(28).

EDSL, 2012. *A-Tas Theory Manual.* [Online]
Available at: http://www.edsl.net/main/support/documentation.aspx
[Accessed 24 July 2013].

EDSL, 2012. *EDSL Tas.* [Online]
Available at: http://www.edsl.net/
[Accessed 09 May 2013].

EnOcean, 2013. *Energy Harvesting Wireless Sensor Solutions and Networks from EnOcean.* [Online]
Available at: http://www.enocean.com/
[Accessed 09 May 2013].

Gustavsen, A. & Berdahl, P., 2003. Spectral emissivity of anodized aluminum and the thermal transmittance of aluminum window frames. *Nordic Journal of Building Physics,* Volume 3.

Helioscreen, 2011. *Helioscreen.* [Online]
Available at: http://www.helioscreen.com.au/
[Accessed 3 September 2013].

ISO, 2003. *ISO 15099:2003. Thermal performance of windows, doors, and shading devices.* Geneva: International Organization for Standardization.

Judkoff, R. N. J., 2006. Model Validation and Testing: The Methodological Foundation of ASHRAE Standard 140. *ASHRAE Transactions,* 112(2), p. 367.

Klaassen, C. J., 2001. Installing BAS sensors properly. *HPAC Engineering,* Issue August 2001, pp. 53-55.

Klems, J., 2002. Solar heat gain through fenestration systems containing shadings: Procedures for estimating performance from minimal data. *ASHRAE Transactions,* 108(1), pp. 512-524.

Klems, J. H., 1994. New method for predicting the solar heat gain of complex fenestration systems- I. Overview and derivation of the matrix layer calculation. *ASHRAE Transactions,* 100(1), pp. 1065-1072.

Klems, J. H. & Kelley, G. O., 1996. Calorimetric measurements of inward-flowing fraction for complex glazing and shading systems. *ASHRAE Transactions,* 102(1), pp. 947-954.

Knauer, T., Kuhn, T. & Platzer, W. J., 2004. Measurement of angle-dependant properties of different solar protection devices. *Proceedings Internationales Sonnenforum,* Volume 2, pp. 2842-2851.

Kotey, N. A., Collins, M. R., Wright, J. L. & Jiang, T., 2009. A simplified method for calculating the effective solar optical properties of a venetian blind layer for building energy simulation.. *Journal of Solar Energy Engineering,* 131(2), pp. 18-27.

Kuhn, T., 2006. Solar control: A general evaluation method for facades with venetian blinds or other solar control systems. *Energy and Buildings,* June(38), pp. 648-660.

Kuhn, T., 2006. Solar control: Comparison of two new systems with the state of the art on the basis of a new general evaluation method for facades with venetian blinds or other solar control systems. *Energy and Buildings,* June(38), pp. 661-672.

Kuhn, T., 2006. Solar control: Comparison of two new systems with the state of the art on the basis of a new general evaluation method for facades with venetian blinds or other solar control systems. *Energy and Building,* June(38), pp. 661-672.

Kuhn, T. E., Bühler, C. & Platzer, W. J., 2001. Evaluation of overheating protection with sun-shading systems. *Solar Energy,* Volume 69, pp. 59-74.

Levermore, G. J., 2008. A review of the IPCC assessment report four, part 1: the IPCC process and greenhouse gas emission trends from buildings worldwide. *Building Services Engineering Research and Technology,* 29(4), pp. 349-361.

Lomanowski, B. A. & Wright, J. L., 2007. Heat transfer analysis of windows with Venetian blinds: a comparative study.. *Proceedings of the 32nd Conference of the Solar Energy Society of Canada (SESCI) and 2nd Conference of the Solar Building Research Network (SBRN).*

Loutzenhiser, P. G. et al., 2007. An empirical validation of modeling solar gain through a glazing unit with external and internal shading screens. *Applied thermal engineering,* 27(2), pp. 528-538.

Mahdavi, A. et al., 2007. Analyzing traditional buildings via empirically calibrated building performance models.. *Proceedings: Building Simulation 2007,* pp. 71-78.

Merriam-Webster, 2013. *Merriam-Webster.* [Online] Available at: http://www.merriam-webster.com/ [Accessed 9 May 2013].

Mills, L. R. & McCluney, W., 1993. The benefits of using window shades. *ASHRAE Journal,* 35(11), pp. 20-26.

Mitalas, G. P. & Stephenson, D. G., 1967. Room thermal response factors. *ASHRAE Transactions,* 73(1), pp. III.2.1-III.2.10.

Nielsen, M. V., Svendsen, S. & Jensen, L. B., 2011. Quantifying the potential of automated dynamic solar shading in office buildings through integrated simulations of energy and daylight.. *Solar Energy,* 85(5), pp. 757-768.

Norford, L. K., Socolow, R. H., Hsieh, E. S. & Spadaro, G. V., 1994. Two-to-one discrepancy between measured and predicted performance of a 'low-energy'office building: insights from a reconciliation based on the DOE-2 model. *Energy and Buildings,* 21(2), pp. 121-131.

Pan, Y., Huang, Z. & Wu, G., 2007. Calibrated building energy simulation and its application in a high-rise commercial building in Shanghai. *Energy and Buildings,* 39(6), pp. 651-657.

Perez-Lombard, L., Ortiz, J. & Pout, C., 2008. A review on buildings energy consumption information. *Energy and buildings,* 40(3), pp. 394-398.

Pfrommer, P., Lomas, K. & Kupke, C., 1996. Solar radiation transport through slat-type blinds: a new model and its application for thermal simulation of buildings. *Solar Energy,* 57(2), pp. 77-91.

Remund, J., Kunz, S. & Schilter, C., 2013. *Handbook of Meteonorm Version 7.0, part II: Theory.* Bern: Meteotest.

Rosenkrantz, T., 2005. *Performance of Energy Efficient Windows and Solar Shading Devices,* s.l.: Licentiate Thesis, Lund University, Lund Institute of Technology.

Saelens, D., Parys, W., Roofthooft, A. & Tablada de la Torre, A., 2013. Assessment of approaches for modeling louver shading devices in building energy simulation programs. *Energy and Buildings,* Volume 60, pp. 286-297.

Sullivan, R., Lee, E. & Selkowitz, S., 1992. A Method of Optimizing Solar Control and Daylighting Performance in Commercial Office Buildings. *ASHRAE Conference Proceedings "Thermal Performance of the Exterior Envelopes of Buildings" V.*

Tahmasebi, F., Zach, R., Schuss, M. & Mahdavi, A., 2012. Simulation model calibration: An optimization-based approach.. *Proceedings of BauSIM 2012: Fourth German-Austrian IBPSA Conference,* pp. 386-391.

Thermokon, 2013. *Thermokon Sensortechnik GmbH.* [Online] Available at: http://www.thermokon.de/ [Accessed 09 May 2013].

Warema, 2013. *Warema Produkte.* [Online] Available at: http://www.warema.at/de-at/Produkte/index.html [Accessed 8 May 2013].

Westphal, F. & Lamberts, R., 2005. Building simulation calibration using sensitivity analysis. *Proceeding of the Ninth International IBPSA Conference,* pp. 1331-1338.

Wiese, M. R., 1982. An analysis of thermal response factors and how to reduce their computational time requirement. *NASA STI/Recon Technical Report*, N, 83: 12523.

Zweifel, G., 2007. New EPDB related European Standards and their relation to building and HVAC system simulation. *Proceedings: Building Simulation 7*.

6.2 Tables

6.3 Figures

Appendix A: Materials and constructions

Table 18: Optical properties of a double glazing, with low emissivity coating on surface 2

Variable	Meaning of the variable	Value
α_1	Direct absorptance of the outer pane, in the	0.26
α'_1	Direct absorptance of the outer pane, in the	0.26
α_2	Direct absorptance of the inner pane, in the	0.20
τ_1	Solar direct transmittance of the outer pane	0.64
τ_2	Solar direct reflectance of the inner pane	0.10
ρ'_1	Solar direct reflectance of the outer pane, in the	0.10
α_{e1}	solar direct absorptance of the outer pane	0.28
α_{e2}	solar direct absorptance of the inner pane	0.13
h_e	Heat transfer coefficients towards the outside	23 W/m².K
h_i	Heat transfer coefficients towards the inside	8,0 W/m².K
Λ	Thermal conductance of the double glazing	1.392 W/m².K
τ_e	Direct solar transmittance of the double glazing	0.452

We obtain g=0.577, like the Tas Construction database, based on EN 410.

Table 19: Slat solar and visual properties for three colours indicated by the manufacturer (Warema 2013)

Colour	Traffic white (RAL 9016)	Light grey (RAL 7035)	Anthracite grey (RAL 7016)
Slat solar transmittance	0.00	0.00	0.00
Slat solar reflectance	0.75	0.52	0.15
Slat solar absorptance	0.25	0.48	0.85
Slat visual reflectance	0.86	0.59	0.08
Slat visual absorptance	0.14	0.41	0.92

Table 20: Solar transmittance and reflectance of external blinds for different colours, and values of slat angle and solar elevation angle α_s, as indicated by the manufacturer (Warema 2013)

Colour	Slat angle	α_s	RAL 9016	RAL 7035	RAL 7016
Blind solar transmittance	45°	30°	0.19	0.12	0.06
Blind solar transmittance	0°	45°	0.35	0.23	0.10
Blind solar reflectance	45°	30°	0.51	0.34	0.09
Blind solar reflectance	0°	45°	0.32	0.19	0.05
Blind solar absorptance	45°	30°	0.30	0.54	0.85
Blind solar absorptance	0°	45°	0.33	0.58	0.85